Methane Conversion to Synthesis Gas over Platinum Supported on Rare Earth Oxides

Thesis by

Piboon Pantu

In Partial Fulfillment of the Requirements

for the Degree of

Doctor of Philosophy

California Institute of Technology

Pasadena, California

2001

(Submitted May 18, 2001)

Acknowledgments

I would like to thank my advisor, Prof. George R. Gavalas, whose insight and creativity have inspired me, for his guidance, support and encouragement throughout the past five years. I also want to thank Prof. Mark E. Davis and Dr. Jay Labinger and Prof. John Seinfeld for reviewing my work and providing helpful comments. I am also very thankful to Prof. Kiseok Kim from Yeungnam University, South Korea, for his interest in my project and constructive discussions.

I am deeply grateful to the DPST scholarship for continuing support throughout my entire education from high school to graduate school. My academic achievement would never be possible without the generous support from the DPST scholarship and people in the DPST project.

I would like to thank everyone in my lab, Re Lai, Beom-Seok Kang, Lixiong Zhang, Huanting Wang, Sun Qi, and Seung-Goo Kim for friendship, and delightful discussions, and great help. I would like to express my appreciation to Neil Fernandes for setting up instruments that I used. I also wish to thank my fellow graduate students, Giyoong Tae, Donald Kuklo, Patrick Piccione, Ganesh Sabramanian, Suzie Hwang, and Lin Luo for bringing out joy and fun even in the most difficult time. Finally, I have found myself very lucky to know Suchada Thaneepanichskul. Her support and companionship have made my life at Caltech more pleasant than I could ever have imagined.

Most of all, the love and support of my parents have made me who I am. No words could express my profound love and gratitude to my mother and father.

Abstract

The central theme of this research is to study methane conversion to synthesis gas focusing on the redox capabilities of cerium oxide.

Reaction of methane with platinum or ruthenium supported on $Ce_{1-x}Zr_xO_2$ ($x=0$, 0.2, 0.5) in the absence of gaseous oxygen was studied in a packed-bed reactor at 550-700°C. The oxidation of methane utilized lattice oxygen of the support, which was subsequently restored by reacting with oxygen in a separate step. Thus, by using the redox property of cerium oxide, methane oxidation can be carried out by air without diluting the product with nitrogen. Addition of ZrO_2 into CeO_2 increased the reducibility of the oxide as well as the rate of methane oxidation but decreased the selectivity to CO and H_2. The rate of oxidation was initially very fast but slowed down as the oxide support became progressively reduced. On the other hand, the selectivity increased with the reduction of the support and sharply rose to over 90% as the support attained 10%, 40%, and 65% degree of reduction for the oxide compositions $x=0$, 0.2, and 0.5, respectively.

Partial oxidation of methane to synthesis gas over 0.5wt% Pt/Al_2O_3 and 0.5wt% Pt/CeO_2 catalysts was studied in a packed-bed reactor. At temperatures up to 650°C, the Pt/CeO_2 catalyst gave higher conversion and higher selectivity but the activity and selectivity became comparable to those of Pt/Al_2O_3 above 700°C. The Pt/CeO_2 catalyst also maintained high conversion and high selectivity when the CH_4:O_2 feed ratio varied from 1.7 to 2.3 while the Pt/Al_2O_3 catalyst had considerably lower selectivity under methane-rich conditions. The effect of reducibility of support on the catalytic activity was discussed.

A multiple microreactor system for parallel testing of heterogeneous catalysts was developed. The reactor system was composed of nine tubular microreactors housed in a single wider tube and used a multiposition valve to conduct the reaction products sequentially from each microreactor to a mass spectrometer for analysis. The catalyst samples were prepared in the form of thin films coated on quartz rods for convenience of preparation and loading samples in the reactors. The system was tested with the reaction of methane reforming with carbon dioxide over $Pt/Ce_{1-x}Gd_xO_{2-0.5x}$ and $Pt/Ce_{1-x}Sm_xO_{2-0.5x}$ at 650°C and 700°C. The measurements showed that Pt/CeO_2 had the highest activity and, generally, the activity increased with cerium oxide content. After exposure to the feed stream for 2-3 hours at 700°C, most catalysts suffered significant deactivation with the exception of the mixed oxides with 25-85% samarium oxide that maintained relatively stable activity.

Table of Contents

List of Tables

List of Figures

Chapter 1

Introduction

1.1 Introduction

Conversion of methane, the major component of natural gas, to useful chemicals and liquid fuels has received much attention due to a strong economic incentive driven by the abundant natural gas supplies. Currently, methane is mainly used as a clean-burning fuel for heating homes, buildings, and also for the generation of electrical power. The use of methane as a chemical feedstock for producing chemicals and liquid fuels is still limited due to its chemical inertness. Moreover, large quantities of methane that are found in remote areas and cannot be economically transported to communities or industrial complexes, are generally reinjected into the resources or flared or vented out which is a waste of the nonrenewable natural resources [1]. To utilize the remote natural gas, methane must be converted to more easily transportable products or liquids of higher value. Besides, with the rapid discovery of global natural gas reserves outpacing growth in oil reserves over the past 20 years [2] and the high crude oil prices nowadays, the production of liquid fuels from methane is becoming more attractive.

Methane can be converted to fuels and useful chemicals by either direct conversion to C_2 and higher hydrocarbons or methanol or by indirect conversion via synthesis gas (a mixture of H_2 and CO). Although the direct conversion is the more desirable route, it is still in an early experimental stage and no viable process has been developed. On the other hand, the indirect route is a much more mature technology. Production of synthesis gas has been commercially operated in large-scale industrial plants by steam reforming of methane.

$$CH_4 + H_2O \leftrightarrows CO + 3H_2 \qquad \Delta H = 206 \text{ kJ/mol} \qquad (1.1)$$

The synthesis gas and hydrogen produced from the steam reforming can be used in many industrial processes, e.g., ammonia synthesis, methanol synthesis, Fischer-Tropsch synthesis of higher hydrocarbons, etc. Although steam reforming is an established process, it requires high investments and high operating costs due to the highly endothermic nature consuming large amounts of energy and requiring high operating pressure and temperature (>900°C). It has been estimated that above 60-70% of the overall cost of the downstream processes is associated with the synthesis gas production [3]. Reduction in the cost of synthesis gas production would have a significant influence on the economics of the downstream processes. Therefore, extensive research effort has currently been carried out to improve the process and reduce the cost of synthesis gas production.

Partial oxidation is an attractive alternative to the conventional production of synthesis gas because it is slightly exothermic and gives a H_2/CO ratio of 2 that is suitable for Fischer-Tropsch and methanol synthesis.

$$CH_4 + \frac{1}{2}O_2 \leftrightarrows CO + 2H_2 \qquad \Delta H = -35\ \text{kJ/mol} \qquad (1.2)$$

However, to avoid high dilution of products by nitrogen partial oxidation requires the use of pure or enriched oxygen, which costs extra investments in air separation plants. The reaction can be carried out with high conversion and high selectivity over noble metal catalysts or Ni catalysts [4-13]. In most catalysts, the reaction involves total combustion followed by reforming of the remaining CH_4 with CO_2 and H_2O [8, 12]. Therefore heat management is an important issue of reactor design for the partial oxidation process to accommodate a large amount of heat released at the front end of the catalyst bed by combustion of methane. In addition, handling of large quantities of undiluted oxygen as well as oxygen-methane mixture requires extra precautions and high safety reactor configurations to reduce explosion hazards. The partial oxidation can also be carried out in a membrane reactor [14-16] where methane and air are passing on the different sides of the membrane. The membrane acts as a barrier preventing direct mixing of air and methane but allows oxygen to penetrate through to react with methane on the other side. Strong research effort is currently under way by industrial and academic groups to develop stable ceramic membranes as well as high activity catalysts and suitable reactor configurations for partial oxidation of methane.

In this research, a two-step process of methane partial oxidation was investigated involving oxidation of methane by a redox oxide catalyst and then regeneration of catalyst in air or oxygen. By separating the two reaction steps, methane is never in direct contact with air or oxygen therefore dilution of product by nitrogen and formation of flammable methane-oxygen mixture can be avoided. For the above reasons, reaction of methane with platinum or ruthenium supported on cerium-zirconium oxide and regeneration of the used catalysts by oxygen were studied in a packed-bed reactor. In addition, methane partial oxidation using gaseous oxygen was also studied over platinum supported on cerium oxide to determine the effect of reducibility of support on the catalytic activity.

Reforming of methane with carbon dioxide has recently regained considerable attention. Fischer and Tropsch [17] were the first to study this reaction in 1928 and showed that most group VIII transition metals had high activities for the reforming reaction.

$$CH_4 + CO_2 \leftrightarrows 2CO + 2H_2 \qquad \Delta H = 247 \text{ kJ/mol} \qquad (1.3)$$

The carbon dioxide reforming has advantages over the steam reforming of producing a lower H_2/CO ratio which is more suitable to Fischer-Tropsch synthesis and providing a useful means of reducing emission of carbon dioxide which is a greenhouse gas. The reaction has a major drawback of rapid catalyst deactivation due to carbon deposition. Although commercial processes for carbon dioxide reforming of methane such as the Calcor Process [18] and the SPARG Process [19] are available, additional research is still needed to develop more stable catalysts with high resistance to coking.

In the last section of this thesis, a multireactor system for parallel testing of heterogeneous catalysts was described. The parallel approach allows large numbers of materials to be systematically synthesized and tested for catalytic activity in a high-throughput fashion thus enhancing the success rate of catalyst discovery. The proposed reactor system consists of nine tubular microreactors operating in parallel. The catalyst samples are in the form of thin films coated on quartz rods for fast sample preparation and convenient sample loading to the reactors. Methane reforming with carbon dioxide over a series of platinum supported on rare earth oxides catalysts was tested in the multireactor system.

1.2 Outline

In Chapter 2, reaction of methane with platinum or ruthenium supported on cerium-zirconium oxides and regeneration of the used catalysts by oxygen were studied in a packed-bed reactor. The effect of metal loading, oxide composition, and surface area were also investigated.

In Chapter 3, methane partial oxidation over platinum catalysts supported on cerium oxide and on aluminum oxide was studied in a packed-bed reactor. The effect of reducibility of the support on the catalytic activity was investigated.

Chapter 4 presents a multireactor system for parallel testing of heterogeneous catalysts. The multireactor system was tested with the reaction of methane reforming with carbon dioxide over platinum supported on mixed rare earth oxides.

References

[1] J.H. Lunsford, Catal. Today 63 (2000) 165.

[2] Energy Information Administration, "Natural gas" *DOE/EIA-0484(2001)* (Washington, DC, March 2001), web site www.eia.doe.gov/oiaf/ieo/nat_gas.html.

[3] M.A. Pena, J.P. Gomez and J.L.G. Fierro, Appl. Catal. A 144 (1996) 7.

[4] A.K. Bhattacharya, J.A. Breach, S. Chand, D.K. Ghorai, A. Hartridge, J. Keary and K.K. Mallick, Appl. Catal. A 80 (1992) L1.

[5] Y. Boucouvalas, Z.L. Zhang and X.E. Verykios, Catal. Lett. 40 (1996) 189.

[6] V.R. Choudhary, A.S. Mamman and S.D. Sansare, Angew. Chem.-Int. Edit. Engl. 31 (1992) 1189.

[7] V.R. Choudhary, B.S. Uphade and A.S. Mamman, Catal. Lett. 32 (1995) 387.

[8] D. Dissanayake, M.P. Rosynek, K.C.C. Kharas and J.H. Lunsford, J. Catal. 132 (1991) 117.

[9] D.A. Hickman, E.A. Haupfear and L.D. Schmidt, Catal. Lett. 17 (1993) 223.

[10] D.A. Hickman and L.D. Schmidt, J. Catal. 138 (1992) 267.

[11] K. Nakagawa, N. Ikenaga, T. Suzuki, T. Kobayashi and M. Haruta, Appl. Catal. A 169 (1998) 281.

[12] M. Prettre, C. Eichner and M. Perrin, Trans. Faraday Soc. 43 (1946) 335.

[13] W.J.M. Vermeiren, E. Blomsma and P.A. Jacobs, Catal. Today 13 (1992) 427.

[14] U. Balachandran, J.T. Dusek, R.L. Mieville, R.B. Poeppel, M.S. Kleefisch, S. Pei, T.P. Kobylinski, C.A. Udovich and A.C. Bose, Appl. Catal. A-Gen. 133 (1995) 19.

[15] S. Pei, M.S. Kleefisch, T.P. Kobylinski, J. Faber, C.A. Udovich, V. Zhangmccoy, B. Dabrowski, U. Balachandran, R.L. Mieville and R.B. Poeppel, Catal. Lett. 30 (1995) 201.

[16] K. Sato, J. Nakamura, T. Uchijima, T. Hayakawa, S. Hamakawa, T. Tsunoda and K. Takehira, J. Chem. Soc.-Faraday Trans. 91 (1995) 1655.

[17] F. Fischer and H. Tropsch, Brennst. Chem. 3 (1928) 39.

[18] S. Teuner, Hydrocarb. Process. 66 (1987) 52.

[19] N.R. Udengaard, J.H.B. Hansen, D.C. Hanson and J.A. Stal, Oil Gas J. 90 (1992) 62.

Chapter 2

Methane Partial Oxidation on Pt/CeO_2-ZrO_2 in the Absence of Gaseous Oxygen

Reprinted with permission from

Appl. Cal. A 193 (2000) 203-214.

Methane Partial Oxidation on Pt/CeO_2-ZrO_2 in the Absence of Gaseous Oxygen

Piboon Pantu, Kiseok Kim*, George R. Gavalas

Division of Chemistry and Chemical Engineering, California Institute of Technology, Pasadena, CA 91125

*School of Chemical Engineering and Technology, Yeungnam University, Kyongsan 712749, South Korea

Abstract

Partial oxidation of methane to synthesis gas over platinum or ruthenium supported on $Ce_{1-x}Zr_xO_2$ (x=0, 0.2 and 0.5) was studied at 550-700°C in the absence of gaseous oxygen. The reaction was carried out in a packed-bed reactor under continuous or pulsed flows of methane. Oxidation utilized oxide oxygen and was initially very fast but slowed down as the oxide support became progressively reduced. Addition of ZrO_2 into CeO_2 considerably increased the rate of methane oxidation and enhanced the reducibility of CeO_2 but decreased the selectivity to carbon monoxide and hydrogen. Specifically it was found that significant production of carbon dioxide and water occurred on the freshly oxidized solid until a certain degree of reduction was reached beyond which the selectivity to carbon monoxide and hydrogen rose to over 90%. This critical degree of reduction was 10%, 40% and 65% for the solid compositions x=0, 0.2, and 0.5 respectively. Additional experiments carried out using carbon monoxide pulses showed

that carbon monoxide oxidation declines sharply and becomes negligible beyond this degree of reduction while oxidation of methane continues much further. Comparison of the two metals showed that platinum is more active but the reaction rate did not change much in the range of platinum loadings of 0.25-1wt%.

2.1 Introduction

Conversion of methane to liquid fuels or chemicals is currently investigated as a means of utilizing natural gas resources, especially remote natural gas that cannot be economically transported by pipeline. The standard commercial process involving steam reforming to synthesis gas followed by Fischer-Tropsch or methanol synthesis is well established but has high capital and operating costs. Considerable research effort is therefore devoted to improving the efficiency of the two major steps, i.e., synthesis gas production and Fischer-Tropsch synthesis. Several direct conversion processes such as oxidative or dehydrogenative coupling to C2 and higher hydrocarbons are also being investigated.

A major thrust in indirect conversion is to replace steam reforming with partial oxidation in the synthesis gas production step. Such partial oxidation can be carried out on supported nickel and other supported metal catalysts with high hydrogen and carbon monoxide selectivities [1-5]. The exothermic rather than endothermic nature of the reaction simplifies reactor and associated equipment although it requires additional safety measures in handling the methane-oxygen reactant stream. An alternative ultrafast partial oxidation on rhodium-coated monoliths or Pt-Rh gauzes provides high selectivities and has the advantage of very compact reactors [6-9]. Either of these two partial oxidation processes must use pure oxygen rather than air to avoid extensive dilution of the product gas by nitrogen that would interfere with the downstream Fischer-Tropsch or other synthesis. The air separation plant required for this purpose is a major component of the overall process cost.

Partial oxidation can also be carried out by passing methane and air at opposite sides of certain ceramic membranes possessing mixed ionic and electronic conductivity. Oxidation of methane takes place by utilizing lattice oxygen which is continuously supplied from the air side of the membrane avoiding mixing of nitrogen with the product stream. A strong effort is currently under way by industrial groups to develop stable ceramic membranes and modules for this promising version of partial oxidation [10-13].

Partial oxidation by redox oxides also permits the use of air rather than oxygen without diluting the product gas with nitrogen. In the first half of the redox cycle, methane is contacted with an oxide like CeO_2 and partially oxidized to a H_2-CO mixture, while in the second half of the cycle the partially reduced oxide is reoxidized with air. By separating the two reactions, methane and air are never brought into direct contact, avoiding nitrogen dilution of the product and formation of flammable mixtures. A similar cyclic redox operation has been commercialized for butane oxidation to maleic anhydride on vanadium-phosphorus oxide using fluidization technology [14].

Cerium oxide is used as an oxygen storage component of automotive catalysts but by itself has very low activity for hydrocarbon oxidation. A metal like platinum can be added to supply the required activity for C-H bond dissociation. The partial oxidation of methane to synthesis gas using CeO_2 as an oxidant was first reported by Otsuka et al. [15-17]. These authors used a mechanical mixture of platinum black powder and low surface area CeO_2 powder (6.3 m^2/g). Because of the limited contact between the two components and the low surface area of CeO_2, the reaction was rather slow and led to rapid carbon formation if continued beyond a 40% degree of CeO_2 reduction to Ce_2O_3. Oxide reoxidation was studied using water or carbon dioxide as oxidants.

In this paper, we report partial oxidation of methane to synthesis gas on platinum supported on high surface area CeO_2 or CeO_2-ZrO_2 solid solutions. Deploying platinum in supported form is obviously necessary for faster reaction and also permits higher utilization of the oxide oxygen without extensive carbon formation. The reaction is studied in continuous and pulsed flows of methane, the latter providing detailed information about the effect of the oxide oxidation state on reaction rate and selectivity. The effects of metal loading, oxide composition, and oxide surface area are also investigated.

2.2 Experimental

2.2.1 Catalyst preparation

Three oxide supports, CeO_2, $Ce_{0.8}Zr_{0.2}O_2$, and $Ce_{0.5}Zr_{0.5}O_2$ were synthesized using the citrate complexation technique [18]. Specified quantities of $Ce(NO_3)_3.6H_2O$ (Alfa, 99.5%), $ZrCl_4$ (Aldrich, 99.9%), and citric acid (Aldrich, 99.5%) in a 1:1 molar ratio of metal ions and acid, were dissolved in water individually, the solutions were mixed, and the mixed solution was evaporated and dried at 70-80°C under vacuum for 4-6 h. The resulting pale yellow foam-like solid was calcined in air at 600°C for 4 h to a fine yellow powder. In order to obtain samples with different surface areas, a sample of cerium oxide was prepared by the method described above but was calcined at 500°C instead. Additionally, a high surface area cerium oxide (Anan Kasei, 99.9%) and a low surface area cerium oxide (Alfa, 99.5%) were also used. Most of the reaction experiments were carried out with samples prepared by the citrate complexation technique and calcined at 600°C, unless indicated otherwise.

The oxide powder was densified and granulated by the following procedure [19]. The powder was mixed with a small amount of water and a measured quantity (4wt% of the oxide powder) of colloidal silica (Aldrich, LUDOX® SM-30) as a binder. The mixture was worked to a dense paste which was wrapped in cloth, placed between two metal plates and compressed by a mechanical vise. Subsequently, the paste was calcined at 600°C for 4 h, crushed and screened to 25-50 mesh (0.7-0.3 mm) powder.

The metal components were added to the granulated oxide supports by incipient wetness impregnation. The metal solutions were prepared by dissolving $Ru(C_5H_7O_2)_3$ (Alfa) or $PtCl_4$ (Alfa, 99.9%) in ethanol and water, respectively. Impregnation was carried out by gradual addition of the metal solution until the solid appeared moistened. The moistened solid was stirred thoroughly and dried at room temperature. The process was repeated until the desired metal loading (0.25-1wt%) was achieved. The resulting solid was dried at room temperature overnight before being calcined at 600°C in air for 4 h.

2.2.2 Catalyst characterization

X-ray diffraction analysis of the catalysts was carried out by a Scintag Pad V diffractometer using Cu-Kα radiation. The specific BET surface area of the samples was measured by nitrogen adsorption at liquid nitrogen temperature using a Micromeritics

ASAP 2000 analyzer. The results of the nitrogen adsorption measurements and XRD analyses are given in Table 2.1 while the X-ray diffraction patterns are shown in Fig. 2.1. The broad peaks indicate small grains, the size of which was estimated using Scherrer's equation. With addition of ZrO_2, the diffracting peaks were shifted to higher 2θ angles. No isolated CeO_2 or ZrO_2 peaks were observed for the $Ce_{0.8}Zr_{0.2}O_2$ and $Ce_{0.5}Zr_{0.5}O_2$ samples, indicating that the quantities of any pure oxides not incorporated in the solid solution were small.

2.2.3 Reactor setup and pretreatment conditions

The reactor consisted of a 4-mm ID quartz tube placed into a vertical, electrically heated tube furnace. A catalyst sample of 0.1 g was placed in the center of the quartz tube and supported at the bottom by a layer of quartz wool and at the top by 0.1 g of 25-35 mesh (0.42-0.7 mm) quartz chips. A thermocouple was attached to the outside surface of the reactor tube and connected to a temperature controller. The reactor was heated up to the reaction temperature (550, 600, 650, or 700°C) with a heating rate of 10°C/min in a flow of oxygen (50 cm^3/min) and the temperature was kept constant throughout the entire experiment. Prior to each experiment the catalyst was pretreated in the oxygen flow at the reaction temperature for 1 h and it was then purged with a flow of inert gas (argon or helium) for 1 h.

2.2.4 Continuous flow experiments

After catalyst pretreatment, flow of the reactant gas consisting of 5% or 20% of methane in helium or argon at 50 cm^3/min was initiated and maintained for 7 minutes.

The catalyst bed was subsequently purged by argon or helium for 10 min at the reaction temperature. Oxygen was then added to the purge stream at 5% by volume to reoxidize the oxide and burn out any deposited carbon. Finally, the catalyst was pretreated again as described above to prepare for a new reaction cycle.

A UTI 100C mass spectrometer was used to analyze continuously the products during the flow of methane and during oxide reoxidation. The measurements of carbon oxides evolved during reoxidation were used to determine the quantity of carbon formed during the preceding methane flow under the assumption that the carbon deposited was completely burnt out in the reoxidation treatment.

2.2.5 Pulse experiments

Methane oxidation and oxide reduction were also studied by passing sequences of methane or carbon monoxide pulses (0.25, 0.5, or 1 cm^3 per pulse) through the catalyst bed. The pulses were carried by helium at 50 cm^3/min flowrate and were separated by 1 min intervals. Each sequence of methane or carbon monoxide pulses was followed by a sequence of oxygen pulses to reoxidize the catalyst and measure the previously deposited carbon. Unconverted reactants and reaction products during pulsing by methane, carbon monoxide, or oxygen were continuously measured with the mass spectrometer.

2.3 Results and discussion

Since ZrO_2 is not reducible at the temperature range studied in this work [20], oxygen supplied for the oxidation of methane derived from reduction of cerium or from any oxygen adsorbed on the surface following the original pretreatment by oxygen flow. The latter possible source of oxygen was neglected on account of the inert purge following that oxidation.

$$2CeO_2 \rightarrow Ce_2O_3 + O \qquad (2.1)$$

$$DR = \frac{[\text{total oxygen release}]}{n_{Ce}/2} \qquad (2.2)$$

Therefore, the calculations were based on the stoichiometry and the oxidation state of the oxide at any time during reaction was characterized by the degree of reduction (DR) defined as the percentage of CeO_2 reduced to Ce_2O_3. In Eq. (2.2) the total oxygen release is given by $n_{CO} + 2n_{CO2} + n_{H2O}$, where n_{CO}, n_{CO2}, n_{H2O} are the cumulative molar quantities of CO, CO_2, and H_2O produced by the reaction and n_{Ce} is the gram-atoms of cerium in the oxide. The amount of water produced was estimated from a hydrogen balance because it could not be quantitatively measured by the mass spectrometer.

The selectivity to carbon monoxide was defined as

$$S_{CO} = \frac{n_{CO}}{n_{CO} + n_{CO2}} * 100 \qquad (2.3)$$

This definition focuses on the definition of the gaseous products. The selectivity with respect to the total products is slightly lower and can be calculated by including the carbon produced.

2.3.1 Continuous flow experiments

The methane oxidation experiments reported in this work are inherently transient since the oxidation level of the solid declines with the consumption of lattice oxygen.

Methane conversion and product evolution decline accordingly and become negligible after 5-10 minutes. The duration of flow experiments was therefore limited to 7 minutes in all runs. Preliminary experiments in our laboratory had shown that oxidation of methane on pure oxide CeO_2 is very slow in agreement with the reports of Otsuka et al. [15-17]. A metal component was, therefore, added as described in catalyst preparation. Three metals were tested for this purpose, nickel, ruthenium, and platinum. Nickel gave rise to a considerably lower activity than ruthenium and platinum, hence, it was abandoned early in the study.

Fig. 2.2 shows transient product concentrations for reaction of 5% CH_4-Ar at 600°C on 0.5% $Ru/Ce_{1-x}Zr_xO_2$ and 0.5% $Pt/Ce_{1-x}Zr_xO_2$. The reactions were initially very fast and produced significant quantities of carbon dioxide and water in addition to the desired products, carbon monoxide and hydrogen. With the decline of the oxidation level of the oxide, methane conversion gradually declined while carbon dioxide and water formation declined more rapidly to a very low level. It is well known that addition of ZrO_2 increases the reducibility of CeO_2 by introducing a defective fluorite structure that enhances oxygen mobility [20]. One would accordingly expect the oxidation rate of methane on CeO_2-ZrO_2 to be faster than on pure CeO_2. The sharper product peaks for CeO_2-ZrO_2 compared to CeO_2 in Fig. 2.2, for both platinum and ruthenium, bear out this expectation. Methane conversion was about the same for reaction on pure CeO_2 and on CeO_2-ZrO_2 but reaction on CeO_2-ZrO_2 was less selective, producing substantial quantities of carbon dioxide and water. Comparison of the two metals shows that platinum has higher activity with the pure CeO_2 support but there is not much difference with the mixed supports. Reaction on ruthenium supported on $Ce_{0.8}Zr_{0.2}O_2$ or $Ce_{0.5}Zr_{0.5}O_2$

appeared to have induction periods of several seconds before evolution of reaction products. As it has been reported that ruthenium supported on rare earth oxide (La, Ce, etc.) is readily oxidized to RuO_2 [21], this delay may be due to the time required to reduce the ruthenium oxide generated in the preceding pretreatment. In view of its higher activity, platinum was chosen for the remaining runs reported below.

2.3.2 Effects of temperature and methane concentration

Fig. 2.3 shows product evolution for reaction of 20% methane in helium at 600°C on three $Pt/Ce_{1-x}Zr_xO_2$ samples. Peak shapes appear to be sharper than in Fig. 2.2, signaling the faster reaction rate and the earlier depletion of oxide oxygen at the higher methane concentration. Table 2.2 lists quantities of products obtained from reactions of 5% and 20% methane at 600°C and 700°C on the Pt/CeO_2 sample. The first cycle of each experiment was conducted with fresh catalyst, while the second cycle was carried out after reoxidation of the oxide and carbon burnout at the reaction temperature. For reaction of the 5% methane mixture, there was a large decrease of product formation from the first to the second cycle. For the mixture containing 20% methane, on the other hand, there was only a slight change from the first to the second cycle. More surprisingly, the degree of reduction and total products formed in the first cycle were higher with the 5% methane mixture. This counterintuitive result may be explained by a faster carbon deposition rate at the higher methane concentration. A more extensive carbon buildup on the metal during reaction of the 20% methane gas caused an early decline of the reaction rate, thereby, preventing CeO_2 from being deeply reduced. Perrichon et al [22] reported that reduction of CeO_2 beyond 60% forms a hexagonal Ce_2O_3 phase that is more difficult to reoxidize. The decline of activity from the first to the second cycle for reaction of the 5% methane mixture could be attributed to the difficulty of fully oxidizing the deeply reduced CeO_2, indicating that complete reoxidation may not be achieved under the regeneration conditions at 600°C.

At 700°C the reaction with 5% methane mixture again yielded a larger amount of products which, however, decreased only slightly from the first to the second cycle. Evidently, regeneration of the deeply reduced oxide at 700°C was almost complete. For the 20% methane mixture, raising the temperature from 600°C to 700°C did not significantly change total product formation except that the deposited carbon increased at the cost of the other products. It appears, therefore, that at high concentration of methane, carbon deposition can suppress the reaction before depletion of the available lattice oxygen. Similar effects of temperature and methane concentration were also observed for the $Ce_{0.8}Zr_{0.2}O_2$ and $Ce_{0.5}Zr_{0.5}O_2$ samples. Carbon deposition would appear to be a problem in industrial application of this catalyst when the feed would be pure methane. However, if a riser/fluidized bed reactor system is used, coking can be kept under control by maintaining a high enough ratio of solid to gas flowrates.

2.3.3 Reaction with carbon monoxide pulses

Fig. 2.4 shows the conversion of successive pulses of carbon monoxide at 600°C and 700°C versus degree of reduction of the oxide. At both temperatures, all samples show very high initial activity for oxidation of carbon monoxide so that the complete conversion was observed. Until a certain degree of reduction has been reached the reaction declines very fast to a very low level. The degree of reduction at which the sharp decrease in the rate takes place increases with the content of ZrO_2 in the oxide. At 600°C, it is approximately 8%, 30%, and 50% for CeO_2, $CeO_{0.8}Zr_{0.2}O_2$, and $Ce_{0.5}Zr_{0.5}O_2$, respectively. At 700°C these values are slightly higher but the effect of ZrO_2 content remains the same.

Regeneration of the samples reduced with carbon monoxide was conducted by passing oxygen pulses at the reaction temperature. Reoxidation was very fast and highly exothermic with full consumption of oxygen in each pulse until the oxide was nearly fully oxidized. No carbon oxides were produced showing that there was no carbon deposition during the preceding reaction with carbon monoxide. The measured oxygen consumption was in good agreement with the amount of carbon dioxide produced during the preceding pulsing with carbon monoxide except for the $Pt/Ce_{0.5}Zr_{0.5}O_2$ sample where oxygen consumption was 10-20% lower than the lattice oxygen consumed in the preceding sequence of carbon monoxide pulses. Part of this difference could be measurement error but it is also possible that the deep reduction of this particular sample prevented full reoxidation.

2.3.4 Reaction with methane pulses

The reaction of 1-cm^3-methane pulses with the three $Pt/Ce_{1-x}Zr_xO_2$ samples was studied at 600°C. For all samples, the reaction started off with relatively high conversion of methane in the first pulse, i.e., 40% for the Pt/CeO_2 sample and 60-70% for the ZrO_2-containing samples (see Fig 2.5a). Afterward, there was a sharp decline of methane conversion from pulse 1 to pulse 2 and a slower decline thereafter. On the other hand the carbon monoxide selectivity rises sharply from very low level to above 90% within the first few pulses. There are pronounced differences between samples with different ZrO_2 content. The samples having higher ZrO_2 content give higher initial methane conversion but lower carbon monoxide selectivity and require a larger number of pulses to bring the selectivity to the 90%+ level. As shown in Fig. 2.5b, where methane conversion is replotted versus degree of reduction, the ZrO_2-containing samples have significantly higher activity and can be reduced further than the Pt/CeO_2 sample. Figure 2.5c summarizes total products up to 40 methane pulses for the three samples, showing that CeO_2 yields higher amount of total products as well as higher selectivity to hydrogen and carbon monoxide.

To determine the effect of degree of reduction on carbon monoxide selectivity, several additional experiments were conducted using 0.25 and 0.5 cm^3 pulse volumes. The results were plotted in Figure 2.6 show that with all samples, the reaction initially results in complete oxidation of methane until a certain degree of reduction has been reached after which the selectivity to carbon monoxide rapidly increases to close to 100%. The degree of reduction at which this rapid selectivity takes place is about 10%, 40%, and 65% for CeO_2, $Ce_{0.8}Zr_{0.2}O_2$, and $Ce_{0.5}Zr_{0.5}O_2$, respectively. It is noted that the rise of carbon monoxide selectivity in the methane pulse experiments (Fig. 2.6) and the decline of carbon monoxide oxidation rate in the carbon monoxide pulse experiments (Fig. 2.4) take place at about the same degree of oxide reduction. Related to these observations is the fact that the oxides can be reduced to a greater extent with methane than with carbon monoxide. For example, at 600°C the Pt/CeO_2 sample could be reduced to 60% with methane while the degree of reduction with carbon monoxide did not seem to exceed 20%.

Fig. 2.7 shows the results of reaction of methane pulses on 0.5% Pt/CeO_2 samples at four different temperatures. The methane oxidation rate and the maximum degree of oxide reduction increase with temperature while the carbon monoxide selectivity is independent of reaction temperature except for the first couple of pulses. Fig. 2.8 shows the cumulative products from 30 methane pulses. Increasing the temperature resulted in increased hydrogen and carbon monoxide production. Carbon dioxide was in all cases very low and did not significantly increase with temperature while water increased substantially but remained as a minor product.

2.3.5 Effect of oxide surface area

Figure 2.9 shows methane conversion and carbon monoxide selectivity versus degree of reduction on four catalysts of 0.5% platinum supported on CeO_2 of different surface areas. Among the three catalysts of surface areas 40, 56, and 112 m^2/g, methane conversion slightly increased and CO selectivity slightly decreased with increasing surface area. However, the catalyst of 4 m^2/g surface area had considerably lower conversion and higher selectivity. The lower activity of that catalyst may have been due to the more severe sintering employed in its preparation as also evidenced by its larger grain size (Table 2.1) or to a lower metal dispersion.

It is known that cerium oxide is susceptible to surface area loss by thermal and, more severely, by chemical treatment [23, 24]. In our experiments, no significant loss of surface area was observed when the samples were heated in air at 600°C. However, there was significant surface area loss after reduction-oxidation cycles. For example, for one of the samples the initial surface area of 40 m^2/g was reduced to 29 m^2/g and 23 m^2/g after 2 cycles of reduction by methane pulses and reoxidation, at 600°C and 700°C respectively. Despite this loss of surface area in the continuous flow experiments, the sample regained most of its initial activity after regeneration at 700°C confirming the relatively weak effect of oxide surface area on the reaction.

2.3.6 Effect of platinum loading

To investigate the effect of platinum loading on the reaction, additional samples of 0.25% and 1% Pt/CeO_2 were prepared and subjected to reaction with methane pulses at 600°C. Interestingly, there was no significant variation in activity among the samples with different platinum loading. Unfortunately, measurement of metal surface area for these catalysts is ambiguous because of considerable hydrogen chemisorption on the oxide. Transmission Electron Microscopy (TEM) characterization of particle size was attempted but, unfortunately, in the TEM micrographs the platinum particles could not be clearly distinguished from the far more abundant small cerium oxide grains. As an alternative characterization we measured the rate of carbon monoxide hydrogenation on the four catalyst samples at 350°C. The major products of this reaction were methane and carbon dioxide as previously reported by Kalakkad et al. [25]. The authors reported that the ratio of carbon dioxide to methane productions from this reaction was found to be very sensitive to the Pt-CeO_2 contact and it increased with the metal dispersion. Unfortunately, the dependence is complicated and not linear so that it can not be used as a direct method to quantify the dispersion of the metal supported. In our experiments the rates came out to be approximately proportional to the metal loading (Fig. 2.10) suggesting that the metal area is also proportional to the loading. Accordingly, the ratio of the rates of carbon dioxide to methane productions does not change much with increasing metal loading implying that the differences in metal dispersion among these samples are not substantial.

The metal loading results and previous studies have demonstrated that methane activation on platinum is relatively fast. Possible rate determining steps are oxidation of chemisorbed carbon at the metal-oxide perimeter, or interface, or diffusion of oxide ions to the metal-oxide interface. In the first alternative the rate should be proportional to the metal-oxide perimeter but this possibility is difficult to reconcile with the relatively constant dispersion suggested by the carbon monoxide hydrogenation experiments. Solid state diffusion as a rate determining step is also difficult to reconcile with the fast reoxidation of the reduced oxides observed in the oxygen pulse experiments. Further work is obviously needed to sort out these issues.

The foregoing discussion may be visualized in the reaction scheme shown in Fig. 2.11. Methane is dissociatively chemisorbed on the metal component in step 1. Dissociation is depicted as a single step although it probably takes place stepwise. The chemisorbed carbon is either oxidized by lattice oxygen (step 2) at or near the contact perimeter between the oxide and platinum particles, or forms an inactive form of carbon. The surface carbon monoxide can either desorb (step 3) or be further oxidized (step 4) with the relative rates of these two reactions controlling the carbon monoxide selectivity. At any given concentration of chemisorbed carbon monoxide the rate of step 3 (desorption rate) is probably insensitive to the oxidation state of the oxide, while the rate of step 4 (further oxidation) decreases rapidly with increasing degree of reduction. As a result, the rapid rise of carbon monoxide selectivity as the oxide support is progressively reduced. A similar argument can be advanced to explain hydrogen selectivity on the basis of the relative rates of steps 5 and 6. The above scheme is plausible but more work is obviously needed to confirm individual steps and settle the previously raised questions about metal loading and oxide surface area.

2.4 Conclusions

Methane partial oxidation takes place readily in the absence of gaseous oxygen by reaction with CeO_2-ZrO_2 containing platinum or ruthenium. Platinum has higher activity although the reaction rate varies little with metal loading in the range 0.25-1%. Likewise variation of the oxide surface area in the range 40-112 m^2/g has only a modest effect on conversion and selectivity. Addition of ZrO_2 to CeO_2 significantly increases the methane oxidation rate and the reducibility of the CeO_2 but decreases the selectivity to carbon monoxide. At high methane concentration, carbon deposition occurs so rapidly that the oxidation reaction is terminated by coking of the metal particles before depletion of available lattice oxygen.

References

[1] D. Dissanayake, M.P. Rosynek, K.C.C. Kharas, J.H. Lunsford, J. Catal. 132 (1991) 117.

[2] V.R. Choudhary, A.M. Rajput, B. Prabhakar, J. Catal. 139 (1993) 326.

[3] M.G. Poirier, J. Trudel, Catal. Lett. 21 (1993) 99.

[4] Y. Chu, S. Li, J. Lin, J. Gu, Y. Yang, Appl. Catal. A 134 (1995) 67.

[5] Y. Boucouvalas, Z. Zhang, X.E. Verykios, Catal. Lett. 40 (1996) 189.

[6] D.A. Hickman, E.A. Haupfear, L.D. Schmidt, Catal. Lett. 17 (1993) 223.

[7] D.A. Hickman, L.D. Schmidt, AIChE J. 39(7) (1993) 1164.

[8] L.D. Schmidt, M. Huff, Catal. Today 21 (1994) 443.

[9] D.A. Goetsch, L.D. Schmidt, Science 271 (1996) 1560.

[10] U. Balachandran, J.T. Dusek, R.L. Mieville, R.B.Poeppel, M.S. Kleefisch, S. Pei, T.P. Kobylinski, C.A. Udovich, A.C. Bose, Appl. Catal. A 133 (1995) 19.

[11] S. Pei, M.S. Kleefisch, T.P. Kobylinski, J. Faber, C.A. Udovich, V. Zhangmccoy, B. Dabrowski, U. Balachandran, R.L. Mieville, R.B. Poeppel, Catal. Lett. 30 (1995) 201.

[12] K. Sato, J. Nakamura, T. Uchijima, T. Hayakawa, S. Hamakawa, T. Tsunoda, K. Takehira, J. Chem. Soc. Faraday Trans. 91(11) (1995) 1655.

[13] M. Alibrando, H.S. Hahm, E.E. Wolf, Catal. Lett. 49 (1997) 1.

[14] M. Rashmikant, US Patent 4 668 802 (1987), to E. I. Du Pont de Nemours and Company.

[15] K. Otsuka, T. Ushiyama, I. Yamanaka, Chem. Lett. (1993) 1517.

[16] K. Otsuka, E. Sunada, T. Ushiyama, I. Yamanaka, Stud. Surf. Sci. Catal. 107 (1997) 531.

[17] K. Otsuka, Y. Wang, E. Sunada, I. Yamanaka, J. Catal. 175(2) (1998) 152.

[18] M.S.G. Baythoun, F.R. Sale, J. Mater. Sci. 17 (1982) 2757.

[19] A.B. Stiles, Catalyst Manufacture, Mercel Dekker, New York, 1983, p. 62.

[20] P. Fornasiero, R. Di Monte, G.R. Rao, J. Kašpar, S. Miriani, A. Trovarelli, M. Graziani, J. Catal. 151 (1995) 168.

[21] L.A. Bruce, M. Hoang, A.E. Hughes, T.W. Turney, J. Catal. 178(1) (1998) 84.

[22] V. Perrichon, A. Laachir, G. Bergeret, R. Fréty, L. Tournayan, J. Chem. Soc. Faraday Trans. 90(5) (1994) 773.

[23] V. Perrichon, A. Laachir, S. Abouarnadasse, O. Touret, G. Blanchard, Appl Catal A 129 (1995) 69.

[24] P. Fornassiero, G. Balducci, R. Di Monte, J. Kašpar, V. Sergo, G. Gubitosa, A. Ferrero, M. Graziani, J. Catal. 164 (1996) 173.

[25] D.S. Kalakkad, A.K. Datye, H.J. Robota, J. Catal. 148 (1994) 729.

Table 2.1 Surface areas, average pore diameter, pore volume from N_2 adsorption, and average grain size from X-ray diffraction of 0.5% Pt/$Ce_{1-x}Zr_xO_2$ samples

Sample	BET surface area (m^2/g)	Average pore diameter (Å)	Pore volume (cm^3/g)	Average grain size (Å)
Pt/CeO_2[a]	40.4	112	0.120	180
Pt/CeO_2[b]	56.4	133	0.193	171
Pt/CeO_2[c]	4	207	0.02	1080
Pt/CeO_2[c]	112	48.2	0.142	108
Pt/$Ce_{0.8}Zr_{0.2}O_2$[a]	58.6	90.0	0.145	73
Pt/$Ce_{0.5}Zr_{0.5}O_2$[a]	41.7	63.7	0.075	59

[a] prepared by citrate complexation and calcined at 600°C

[b] prepared by citrate complexation and calcined at 500°C

[c] commercial samples

Table 2.2 Products of reaction of gas mixtures with 5% and 20% CH_4 in He on 0.5% Pt/CeO_2 samples at 600°C and 700°C.

Temperature (°C)		600				700			
CH_4 feed (%)		5		20		5		20	
Cycle number		1	2	1	2	1	2	1	2
	H_2	303	204	262	256	341	314	260	257
Products	CO	139	97	117	114	156	150	111	109
(μmol)	CO_2	8.7	5.6	6.8	7.4	9.3	7	7.8	8.3
	H_2O	14	7.9	4.7	6.1	9.7	8.9	5.0	7.3
	Carbon	9.9	3.5	9.7	9.5	10	4.6	13	14
CO selectivity (%)		94.1	94.6	94.5	93.9	94.4	95.5	93.5	92.9
DR (%)		58.8	39.9	46.6	46.5	63.4	59.5	45.6	46.0

Reaction conditions: 0.1 g catalyst, total flow rate 50 cm^3 /min, reaction time 7 min

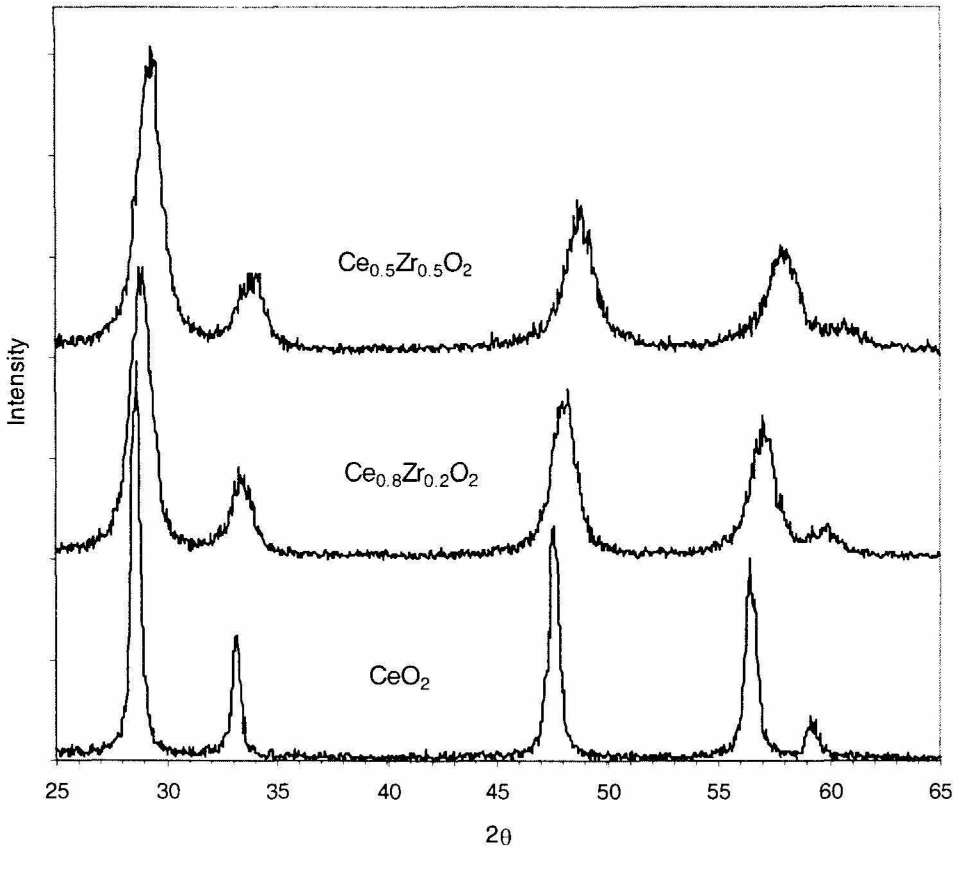

Figure 2.1 X-ray diffraction patterns of $Ce_{1-x}Zr_xO_2$ samples.

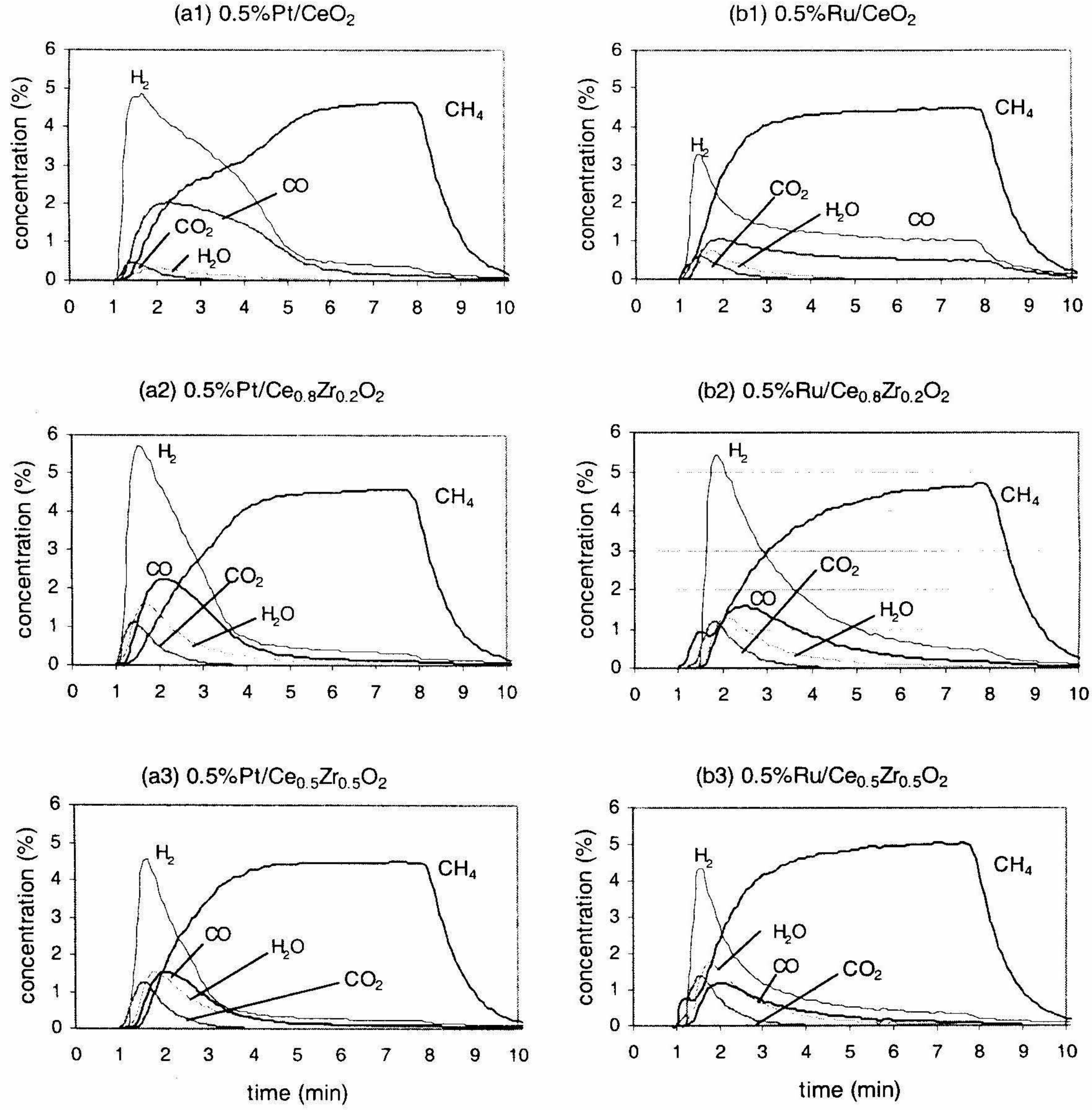

Figure 2.2 Transient product composition in the reaction of 5% CH_4-Ar with 0.5% $Pt/Ce_{1-x}Zr_xO_2$ and 0.5% $Ru/Ce_{1-x}Zr_xO_2$ at 600°C.

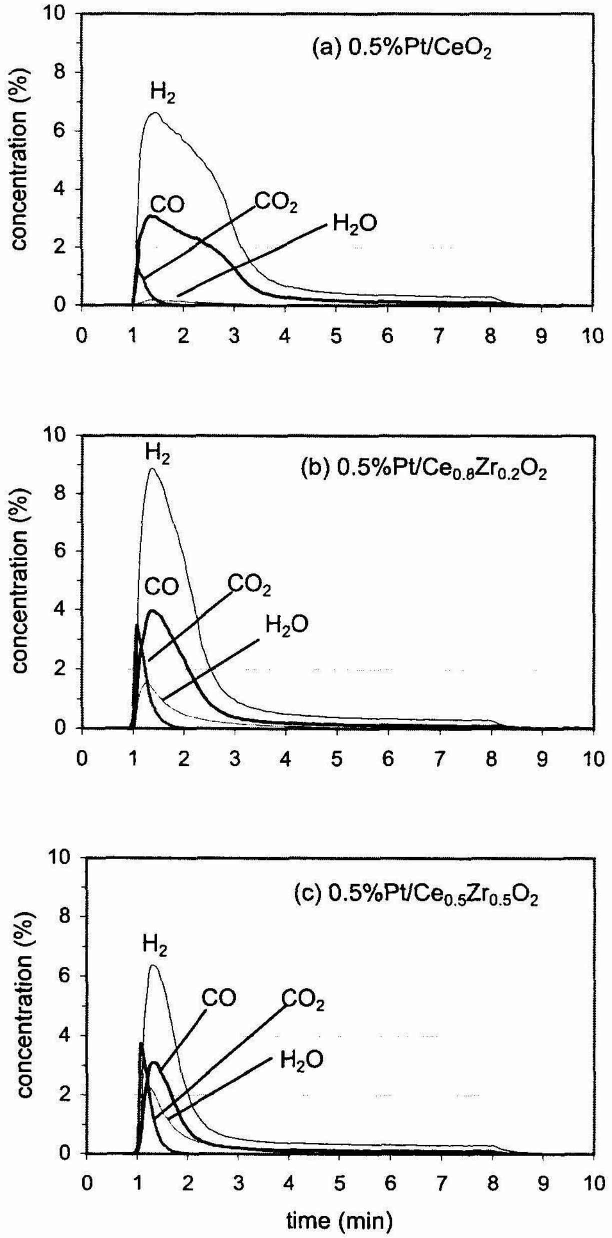

Figure 2.3 Transient product composition in reaction of 20% CH_4-He with 0.5% Pt/$Ce_{1-x}Zr_xO_2$ at 600°C.

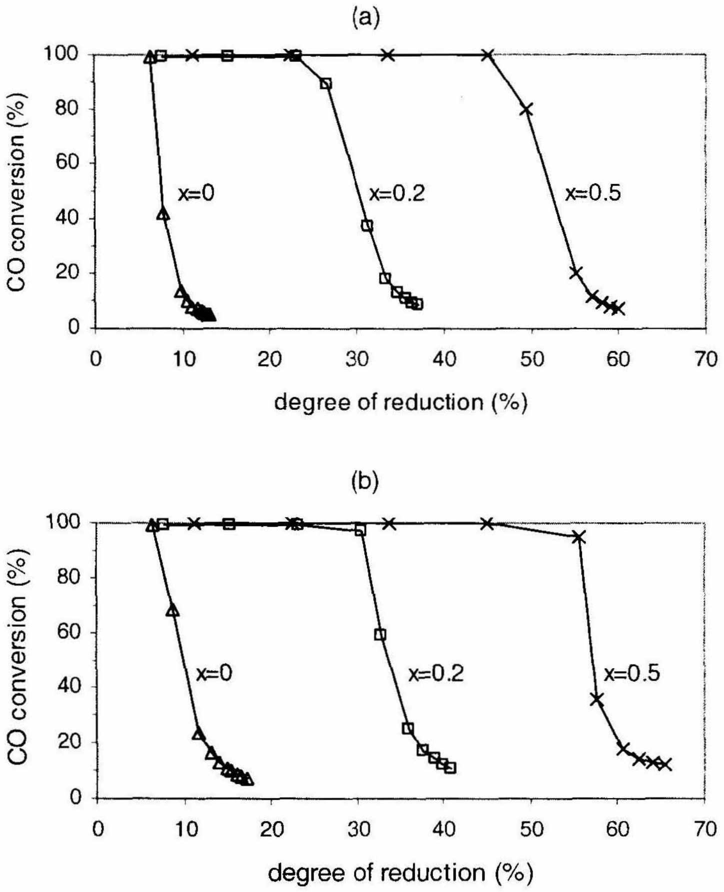

Figure 2.4 Results of reduction of 0.5% Pt/$Ce_{1-x}Zr_xO_2$ by a sequence of 0.5 cm^3 CO pulses at (a) 600°C and (b) 700°C.

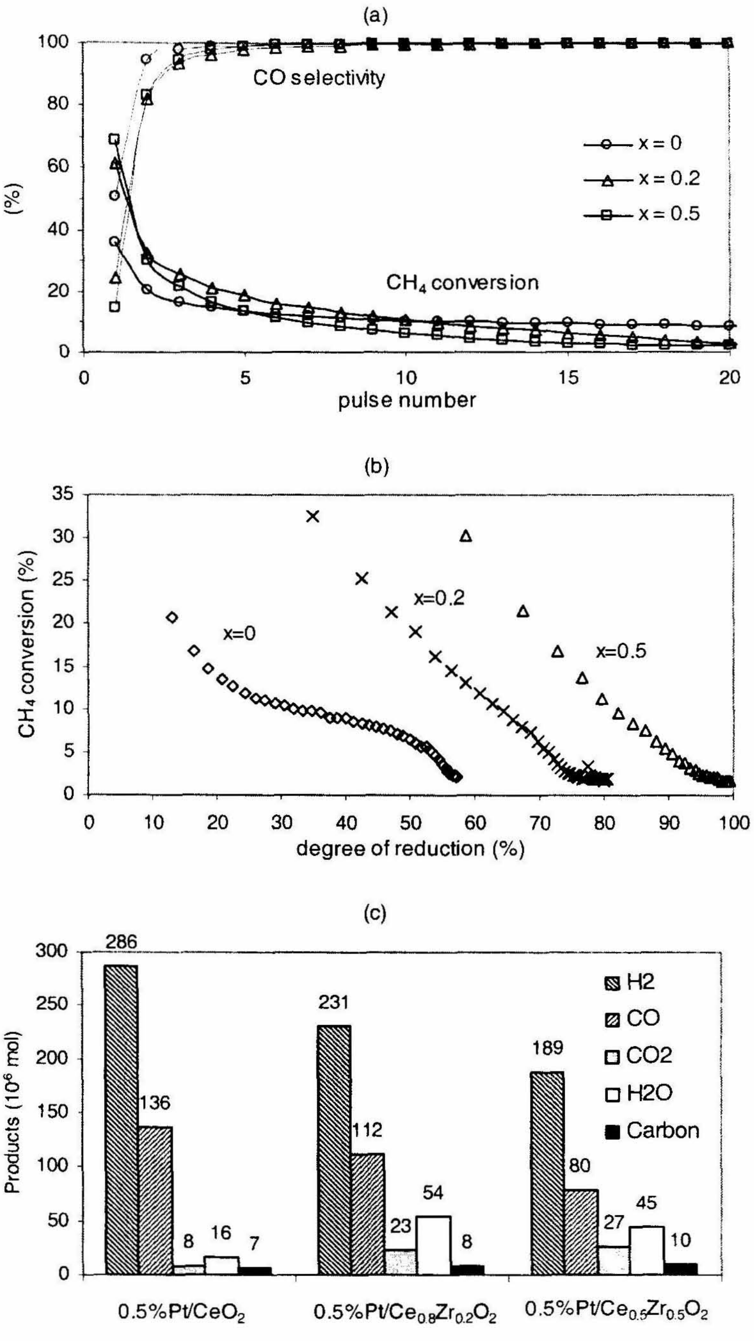

Figure 2.5 Results from reaction of a sequence of 1 cm^3 CH_4 pulses with 0.5% $Pt/Ce_{1-x}Zr_xO_2$ (x=0, 0.2, and 0.5) at 600°C (a) CH_4 conversion and CO selectivity vs. pulse number (b) CH_4 conversion vs. degree of reduction (c) Cumulative products from reaction with 40 pulses of CH_4.

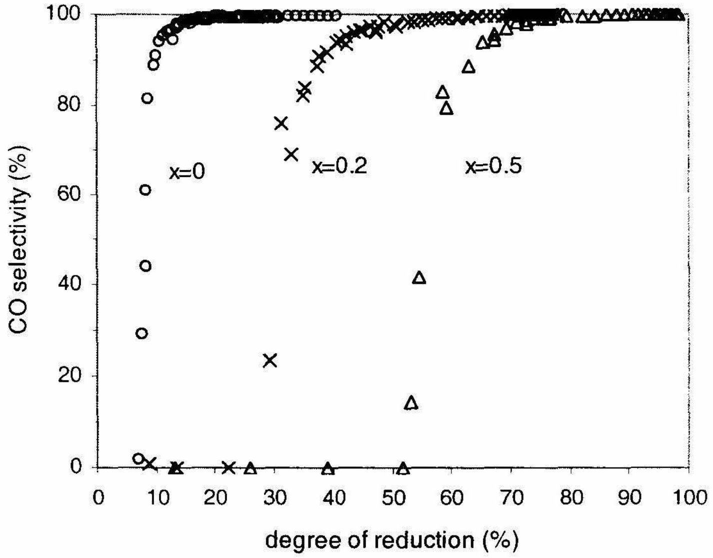

Figure 2.6 CO selectivity vs. degree of reduction in reaction of methane pulses (0.25, 0.5, 1 cm^3) with 0.5% $Pt/Ce_{1-x}Zr_xO_2$ at 600°C.

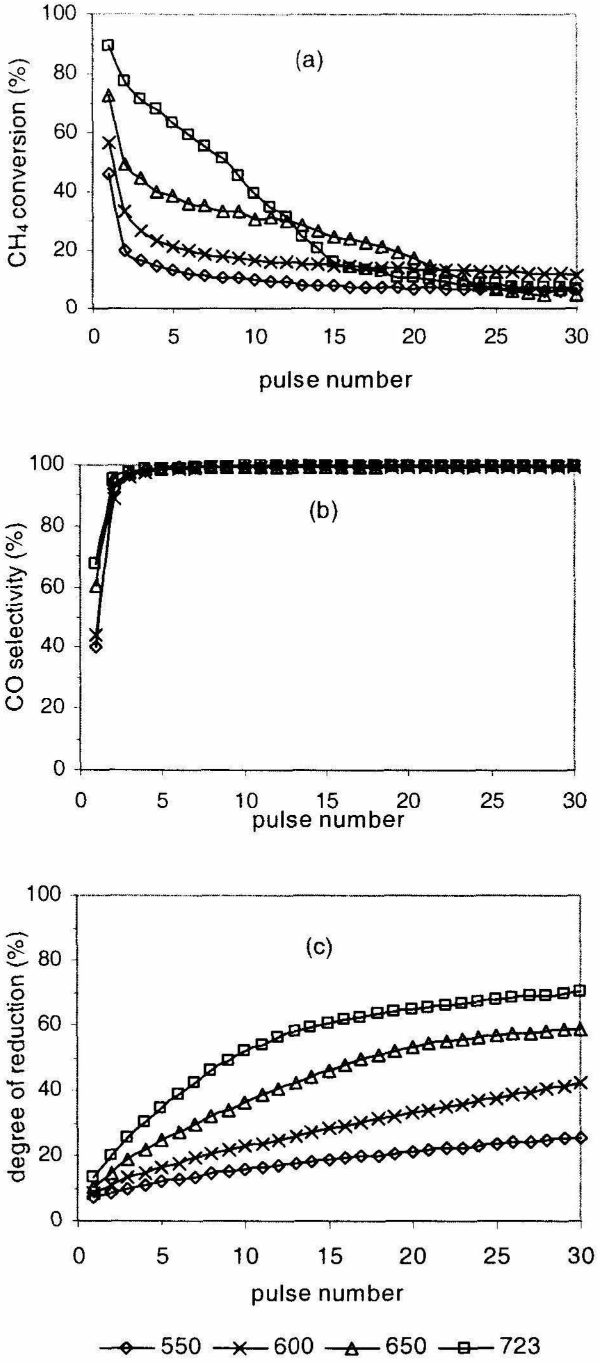

Figure 2.7 Results from reaction of 0.5 cm^3 pulses of CH_4 with 0.5% Pt/CeO_2 at 550, 600, 650 and 723°C.

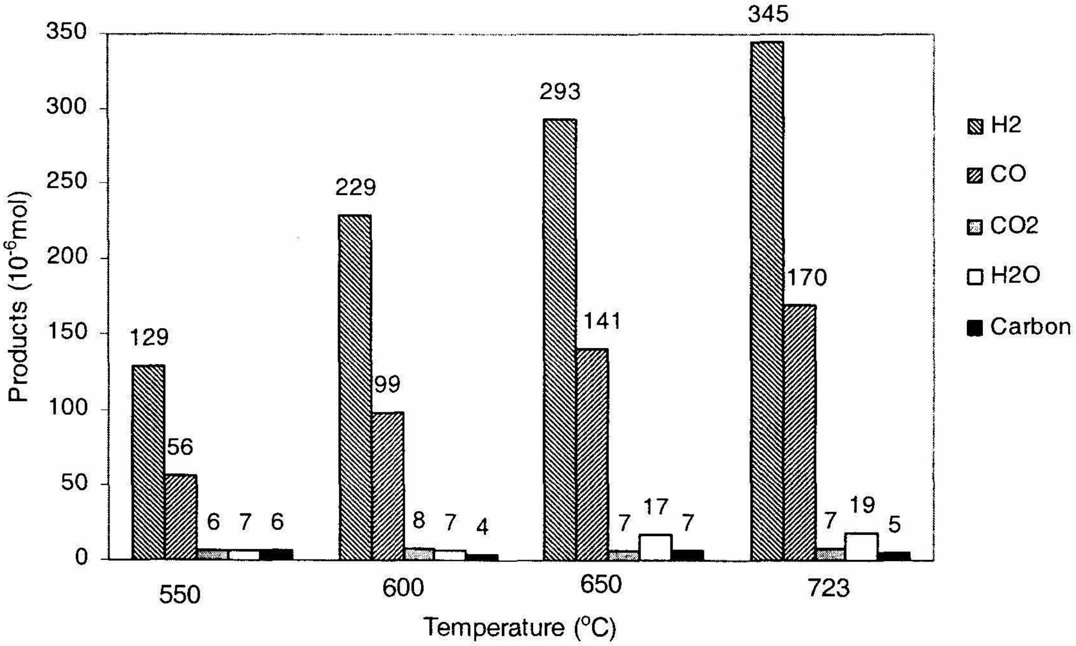

Figure 2.8 Cumulative products from 30 0.5-cm^3-pulses of CH_4 reacting with 0.5% Pt/CeO_2 at different temperatures.

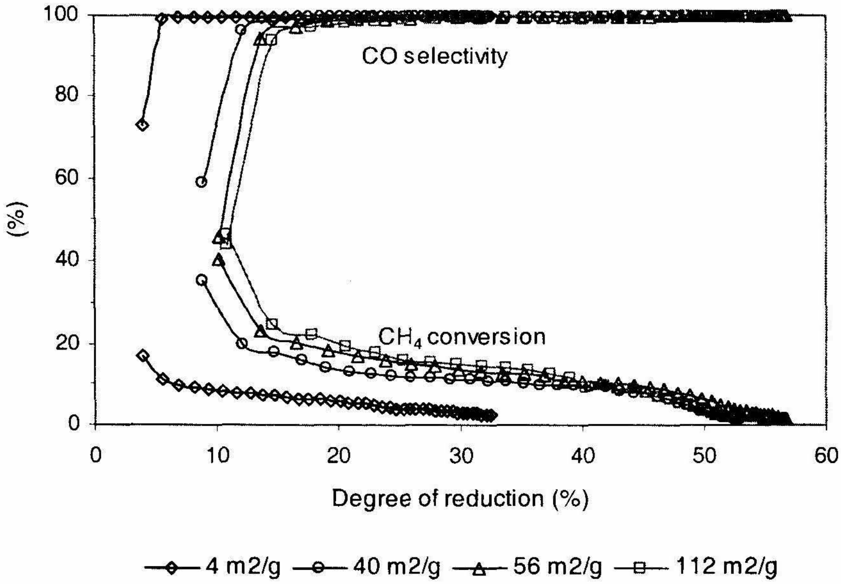

Figure 2.9 CO selectivity and CH_4 conversion at 600°C from a sequence of 1 cm^3 CH_4 pulses vs. degree of reduction of 0.5% Pt/CeO_2 samples of different surface areas.

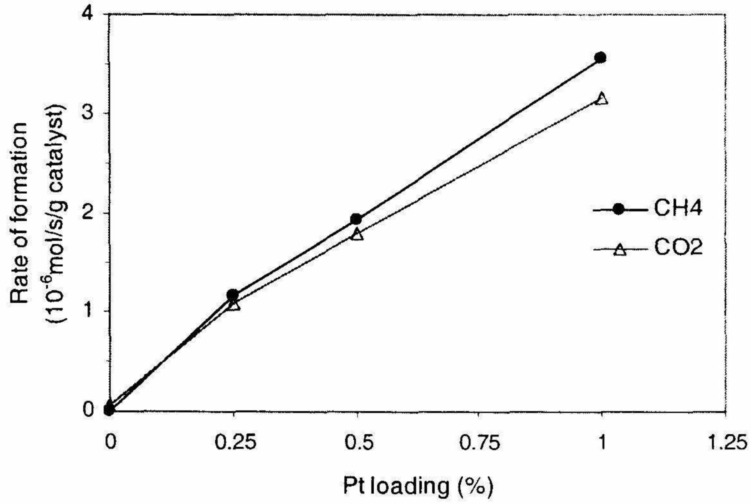

Figure 2.10 Rate of CO hydrogenation at 350°C on Pt/CeO_2 with different Pt loadings (reaction conditions: 0.1 g catalyst: feed gas 67He-25H_2-8CO volume% at 60 cm^3/min).

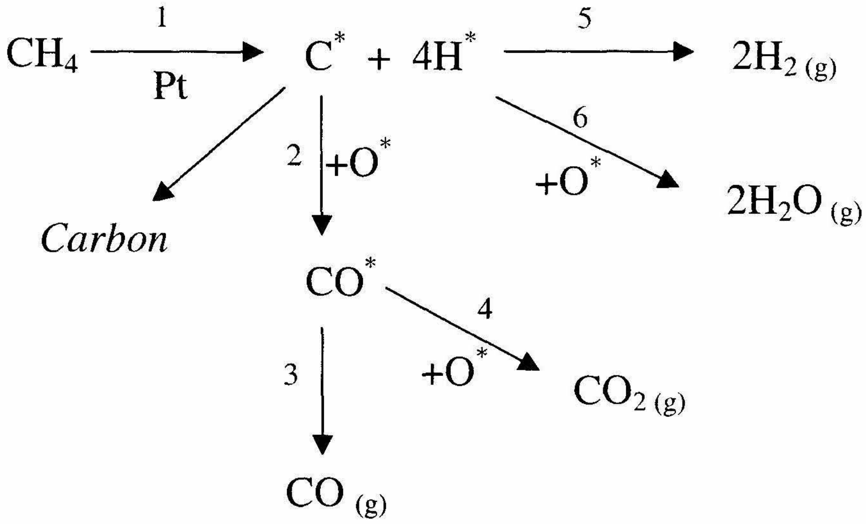

Figure 2.11 Suggested reaction network for methane oxidation on Pt/$Ce_{1-x}Zr_xO_2$ (Stars indicate surface species).

Chapter 3

Methane Partial Oxidation on Pt/CeO_2 and Pt/Al_2O_3 Catalysts

Submitted for publication in Applied Catalysis A: General

Methane Partial Oxidation on Pt/CeO_2 and Pt/Al_2O_3 Catalysts

Piboon Pantu and George R. Gavalas

Division of Chemistry and Chemical Engineering, California Institute of
Technology, Pasadena, CA 91125

Abstract

Partial oxidation of methane to synthesis gas over 0.5wt% Pt/Al_2O_3 and 0.5wt% Pt/CeO_2 catalysts was studied in a packed-bed reactor and supplementary runs of methane reforming with carbon dioxide were carried out. Fresh and used catalysts were characterized by nitrogen adsorption (BET method) for total surface area, and by H_2 and CO chemisorption or by the rate of propene hydrogenation for metal surface area. At temperatures up to 650°C, the Pt/CeO_2 catalyst gave considerably higher methane conversion and higher selectivity to CO and H_2 but above 700°C, the activities and selectivities of both catalysts were comparable. The Pt/CeO_2 catalyst maintained high selectivity to CO and H_2 when the CH_4:O_2 feed ratio varied from 1.7 to 2.3 while the Pt/Al_2O_3 catalyst had lower activity and selectivity under methane-rich conditions. The Pt/CeO_2 catalyst was also more active for methane reforming by carbon dioxide.

3.1 Introduction

Catalytic partial oxidation of methane to synthesis gas is an attractive alternative to steam reforming for production of synthesis gas. The exothermic nature of partial oxidation makes the process less energy and capital cost intensive than the conventional endothermic steam reforming, and the lower H_2/CO ratio of about 2 is more favorable with respect to downstream processes such as methanol synthesis and Fischer-Tropsch synthesis of higher hydrocarbons.

$$CH_4 + 1/2O_2 \rightarrow CO + 2H_2 \quad \Delta H = -36\,\mathrm{kJ/mol} \qquad (3.1)$$

Several supported noble metals (Rh, Pt, Ru, Pd) or Ni catalysts have given high conversion and high selectivity to CO and H_2 [1-10]. Although the supports used in these studies were mainly irreducible oxides such as Al_2O_3, SiO_2, MgO, etc., use of reducible oxides could result in additional process benefits.

Cerium oxide has been used in automotive exhaust catalysts (three-way catalyst, TWC), typically consisting of Pt, Pd, and Rh supported on alumina pellets, or monolith containing a small amount of cerium oxide. In these catalysts, cerium oxide primarily serves as an oxygen storage component [11-12] ensuring stable conversion during the oxygen rich/lean oscillation of the exhaust gas composition. In addition, cerium oxide hinders the thermally induced sintering of the support [13-14], stabilizes the metal dispersion [15-16], and promotes the water gas shift reaction at relatively low temperatures [17-20]. In a series of publications [21-23], Gorte and coworkers reported that noble metals (Pd, Pt, Rh) had much higher specific rates for water gas shift, steam reforming, and carbon dioxide reforming of methane when supported on cerium oxide than when supported on silica or alumina. They pointed out that the advantage of cerium oxide as a support was due to its reducibility and proposed that the reactions involved a bifunctional mechanism in which oxygen from cerium oxide reacts with carbonaceous species adsorbed on the noble metal while the partially reduced cerium oxide is simultaneously reoxidized by the gaseous oxidant.

The reducibility of cerium oxide could also be useful for the partial oxidation of methane on supported metal catalysts. Otsuka et al. [23-26] were the first to show that cerium oxide could partially oxidize methane to synthesis gas, in the absence of gaseous oxygen, and that addition of small quantities of platinum powder could greatly enhance the rate of oxidation. In a previous publication [27], we reported results on methane partial oxidation by direct reaction with Pt/CeO_2 catalysts. The selectivity of the reaction to CO and H_2 increased with the degree of reduction of the cerium oxide support and exceeded 90% after 10% of CeO_2 was reduced to Ce_2O_3. Re-oxidation of the reduced cerium oxide was in all cases very fast.

Because of its fast reduction and oxidation, cerium oxide may also be a useful support for the partial oxidation of methane by gaseous oxygen and the reforming of methane with carbon dioxide. However, Ruckenstein and Wang [28] recently reported that rhodium supported on irreducible oxides was more active and more stable for methane partial oxidation than rhodium supported on reducible oxides (including cerium oxide). The authors suggested that the lower activity in the case of the reducible supports was due to partial coverage of rhodium sites by migration of the partially reduced oxide during the reaction and the lower selectivity resulted from fast combustion of methane on the reducible oxides. In this paper we reexamine the issue of reducible versus irreducible supports for partial oxidation of methane for the case of platinum rather than rhodium catalysts.

3.2 Experimental

3.2.1 Catalyst preparation

Cerium oxide supports were prepared using the citrate complexation technique [29]. Equal molar quantities of $Ce(NO_3)_3 \cdot 6H_2O$ (Alfa, 99.5%) and citric acid (Aldrich, 99.5%) were dissolved in water separately. The solutions were mixed and dried in a vacuum oven at 70-80°C for 4-6 h resulting in an amorphous foam-like precursor that was subsequently calcined in air at 600°C for 4 h to a fine oxide powder. The oxide powder was mixed with a small amount of water and a measured quantity (4wt% of the oxide powder) of colloidal silica (Aldrich, LUDOX® SM-30) as a binder, pressed to a dense paste, dried and calcined at 600°C for 4 h. The calcined solid was crushed and sieved to 50-100 mesh (0.2-0.3 mm). An aluminum oxide sample (Harshaw/Filtrol, γ-Al_2O_3) was also crushed and sieved to the same size. Platinum was added to the oxide supports by incipient wetness impregnation with a solution of $PtCl_4$ (Alfa, 99.9%). The impregnated oxides were dried and calcined in air at 600°C for 4 h. The final Pt/CeO_2 and Pt/Al_2O_3 catalysts had surface areas of 40 and 268 m^2/g, respectively, and both contained 0.5wt% platinum.

3.2.2 Reactor setup and sample pretreatment procedure

Partial oxidation of methane was studied in a tubular quartz reactor (ID 4 mm). A 50-mg sample was placed in the middle of the reactor supported at the bottom with a quartz wool plug and at the top covered with 100 mg quartz chips (50-100 mesh). The catalyst bed lengths were 3 and 6 mm for Pt/CeO_2 and Pt/Al_2O_3 samples, respectively. A mass spectrometer (UTI 100C) was used in all experiments to measure the composition of the product gas. Before using in reaction experiments, fresh Pt/CeO_2 samples were heated to the reaction temperature in oxygen flow (50 ml/min) and kept at that flow for 1 h. The reactor was then purged with helium (50 ml/min) for 1 h to remove gaseous and adsorbed oxygen before switching to the reactant flow. Fresh Pt/Al_2O_3 samples were heated to the reaction temperature in flow of 15%H_2-He (60 ml/min) and kept in that flow for 1 h before switching to the reactant flow.

3.2.3 Methane partial oxidation

In the first set of experiments, the feed was undiluted CH_4-O_2 mixture in 2:1 ratio at total flow rate 110-120 ml/min. Measurements were carried out at furnace temperature adjusted sequentially to 400, 500, and 600°C. At each reaction temperature, the rate was measured every 15 minutes until steady state was achieved (usually it took 1-1.5 h) after which the temperature was raised to the next level at 6.6°C/min heating rate.

In another set of experiments, the rate of methane partial oxidation was measured at 600-700°C for diluted feed (CH_4:O_2:He = 2:1:17) at total flow rate 50 ml/min. At each temperature, product composition was measured every 20 min for 3 h after which the reactant flow was replaced by helium flow at 50 ml/min. Subsequently three oxygen pulses (0.5 ml each pulse) were passed through the reactor at a one-minute intervals. Oxygen consumption and carbon oxides production were measured using the mass spectrometer.

3.2.4 Carbon dioxide reforming of methane

Supporting experiments on reforming of methane with CO_2 were carried out at 600 and 700°C by passing a stream of 10% CH_4, 10% CO_2, balance helium through the pretreated catalysts at total flow rate 50 ml/min. The transient product composition was measured until steady state was reached in about 1-1.5 h.

3.2.5 Catalyst characterization

-Total surface area

The BET surface areas of catalysts were measured by nitrogen adsorption at liquid nitrogen temperature using a Micromeritics ASAP 2000 analyzer. The surface areas were measured for the fresh catalysts and for the catalysts exposed to the diluted feed at 700°C for 2 h.

-Platinum dispersion

Platinum dispersion on the alumina-supported catalysts was estimated from H_2 and CO chemisorption at room temperature assuming a 1:1 stoichiometry for both gases and a hemispherical shape of the platinum particles. For this purpose, a 100-200 mg catalyst sample was packed in a tubular quartz reactor and reduced in hydrogen flow (50 ml/min) at 500°C for 1h. The reactor was then purged by helium flow (50 ml/min) and cooled down to room temperature. Subsequently, pulses of CO (100 μl per pulse) or pulses of H_2 (25 μl per pulse) were passed through the catalyst until no further adsorption was detected. A gas chromatograph equipped with a thermal conductivity detector and a mass spectrometer were used to measure CO and H_2 concentrations at the outlet.

Platinum dispersion on catalyst supported on cerium oxide could not be estimated from H_2 or CO chemisorption because both gases adsorb on cerium oxide. Instead, an indirect method based on the rate of propene hydrogenation was employed. The rate of this structurally insensitive reaction was measured at 0°C under differential conditions. A catalyst sample of 10-50 mg mixed with 100 mg of quartz chips was packed in the middle of a tubular quartz reactor (ID 4 mm) and reduced in hydrogen flow at 500°C as described above. After cooling down to 0°C, a flow of 10% propene and 10% hydrogen in helium (50 ml/min) was passed through the reactor and product composition was measured using the mass spectrometer. The rate of propene hydrogenation was also measured on the Pt/Al_2O_3 catalysts. Thus a conversion factor was established for the alumina-supported catalysts between H_2 chemisorption and the rate of propene hydrogenation. This conversion factor was also used for the catalyst supported on the cerium oxide assuming that the specific rate of hydrogenation was independent of the support.

3.3 Results and discussion

3.3.1Catalyst characterization

The BET surface areas and platinum dispersion of the Pt/CeO_2 and Pt/Al_2O_3 catalysts are presented in Table 3.1. As freshly prepared, Pt/CeO_2 had a higher propene hydrogenation rate than Pt/Al_2O_3 suggesting somewhat higher dispersion of Pt/CeO_2 despite of the lower support surface area. After being used in methane partial oxidation at 700°C, both catalysts lost surface area but the Pt/CeO_2 catalyst suffered more severe loss. The propene hydrogenation activity of Pt/CeO_2 was also drastically reduced indicating large loss of accessible platinum. On the other hand, the propene hydrogenation activity of Pt/Al_2O_3 did not change much indicating a smaller extent of sintering. The adsorption of CO and H_2 on Pt/Al_2O_3 also showed only small decline after reaction at 700°C consistent with the propene hydrogenation rate. The catalysts exposed to reaction at 600°C had very similar propene hydrogenation rates suggesting comparable dispersion of platinum on both supports.

3.3.2 Catalytic activity

The results of experiments using the undiluted reactant mixture are shown in Table 3.2. In this set of experiments, the furnace temperature was set to a relatively low level (400-600°C) to compensate for the large amount of heat released. As reported by Dissanayake et al. [30], at high flow rate of the CH_4-O_2 feed, a steep hot spot developed inside the catalyst bed making it very difficult to define or measure a reaction temperature. In the present experiments, the temperature inside the catalyst bed was 400-

500°C higher than the furnace temperature and when using the Pt/Al_2O_3 catalyst there was a temperature difference of 200°C or more along the catalyst bed. Under these conditions, a single reaction temperature could not be defined and the furnace temperature was used only to characterize the reactor operation. Although an unambiguous comparison of the two catalysts is impossible under these conditions, qualitative trends about activity and selectivity could be observed. Increasing the temperature resulted in higher methane conversion and CO and H_2 selectivity for both catalysts. Small increases of the oxygen content in the feed stream (CH_4/O_2 = 1.9 to 1.7) also resulted in higher methane conversion but the selectivity remained unchanged. Under oxygen-deficient conditions (CH_4/O_2 feed ratio 2.3), on the other hand, the Pt/CeO_2 catalyst maintained high CO and H_2 selectivity but the Pt/Al_2O_3 catalyst gave significantly lower conversion and somewhat lower selectivity. It was also found that the Pt/CeO_2 catalyst had significantly higher selectivity for H_2 than for CO. No visible carbon deposit appeared on the Pt/CeO_2 catalyst over the range of feed compositions examined, but the Pt/Al_2O_3 catalyst became darker under methane-rich conditions indicating some coke deposit which, however, was not measured.

To examine the effect of reaction temperature on methane oxidation it was necessary to avoid the development of a hot spot. Accordingly, in the second set of experiments the feed was diluted with helium and the flow rate was reduced. The $CH_4:O_2$ feed ratio in these experiments was kept in the range 1.8-2. Table 3.3 presents the results of runs using diluted feed and compares them with constrained equilibrium values (excluding carbon formation and fixing the value of the $CH_4:O_2$ feed ratio at the nominal value of 2). In all experiments oxygen was completely consumed. At 600°C, the Pt/CeO_2

catalyst gave significantly higher methane conversion and higher selectivity to CO and H_2 but the activity and selectivity of both catalysts were still far below the equilibrium values. Replicate runs gave less than 10% relative error on conversion and selectivity. Also, variation of the CH_4:O_2 ratio within the indicated range (1.8-2) gave small changes in conversion and selectivity. Therefore, the larger differences in activity and selectivity of the catalysts at 600°C can be attributed to the different properties of the catalysts. At 700°C, the activity of both catalysts became comparable and the product composition approached equilibrium.

As mentioned in the experimental part, the packed bed of the alumina-supported catalyst was twice as long as the bed of the higher density ceria-supported catalyst. Although the space velocities with respect to platinum were the same for both catalysts, the different bed lengths raised the possibility of different temperature distributions resulting from the exothermic reaction and influencing the comparisons of activity and selectivity. To test that possibility an additional experiment was carried out in which the Pt/CeO_2 catalyst was mixed with quartz chips to double the bed length. The results showed no significant difference between the diluted and the undiluted catalysts indicating that the different bed lengths were not a significant factor in the results obtained with the helium-diluted feed.

During regeneration by oxygen pulses, only small quantities of carbon oxides were produced indicating in all cases negligible carbon deposition (less than 0.006% of methane converted). Oxygen consumption during regeneration was negligible in the case of the Pt/Al_2O_3 catalysts but considerable for the Pt/CeO_2 catalysts resulting from re-oxidation of the partially reduced cerium oxide. By assuming that reaction with oxygen can completely oxidize the oxide support, the degree of reduction (DR) is defined as the quantity

$$\mathrm{DR}\ (\%) = 100[\text{oxygen uptake}]/(n_{Ce}/2), \qquad (3.2)$$

where n_{Ce} is the gram equivalents of cerium in the catalyst, and oxygen uptake is the atomic oxygen consumption minus the atomic oxygen in the oxygenated products. With this definition, DR=0 corresponds to CeO_2, DR=100 corresponds to Ce_2O_3, and intermediate DR correspond to nonstoichiometric CeO_{2-x}. In the case of the Pt/CeO_2 catalyst, selectivity to CO and H_2 increased with degree of reduction and both selectivities increased with reaction temperature, consistent with our previous results [27].

Additional experiments with very short catalyst beds (10 mg) were carried out at 600°C and 700°C (Table 3.4). Despite the small amount of catalyst and the very short bed length (ca. 1 mm), oxygen conversion was 100% for both catalysts. However, methane conversion and selectivity to CO and H_2 were significantly lower than in the experiments conducted using 50 mg of catalyst. These results suggest that fast methane oxidation depletes gaseous oxygen in the front section of the catalyst bed after which the CO_2 and H_2O products further react with methane resulting in additional methane conversion and CO and H_2 production. Since methane oxidation by gaseous oxygen was fast on both catalysts, the different activities must be attributed to the methane reforming by CO_2 and H_2O after oxygen was completely consumed.

Separate runs of methane reforming with CO_2 were carried out, and as shown in Table 3.5, reforming on Pt/CeO_2 at 600°C was about two times faster than on Pt/Al_2O_3. At 700°C, the difference in the reforming activity of both catalysts became less pronounced as the products approached equilibrium. A number of previous reports also showed that methane reforming with CO_2 or H_2O over noble metals supported on cerium oxide were faster than over the metals supported on aluminum oxide [17-23]. The faster reforming on cerium oxide-supported catalysts is likely due to the utilization of lattice oxygen from the oxide support and reoxidation of the lattice by gaseous CO_2 and H_2O as previously reported in the literature [21-23]. Finally, the values of H_2:CO ratio higher than 2 measured at the lower temperatures suggest that on Pt/CeO_2 methane reforming with water is faster than reforming with CO_2, consistent with a previous report [25] that water is a better oxidizer for the partially reduced cerium oxide.

The faster reforming reactions on Pt/CeO_2 could explain the higher methane conversion and higher selectivity to CO and H_2 obtained with that catalyst in the partial oxidation of methane at 600-650°C. The redox reactions of cerium oxide with CH_4 and CO_2 or H_2O at or near the $Pt-CeO_2$ interface are expected to be important in steady state partial oxidation of methane, especially in the downstream section of the catalyst bed where there is no gaseous oxygen.

Ruckenstien and Wang [28] previously reported that rhodium supported on reducible oxides had much lower activity and selectivity for partial oxidation of methane than rhodium on irreducible oxides. The difference was attributed to partial coverage of rhodium sites by the reducible oxides and the high total combustion activity of the reducible oxides. It should be noticed, however, that the reducible oxides used in their study had very low surface areas (less than 5 m^2/g). Moreover, the rhodium surface areas of the reducible oxides were approximately one order of magnitude lower than those of the irreducible oxides. Thus, the lower activity of rhodium supported on the reducible oxides could be due to their lower support and metal surface areas. Different metal-support interactions between Rh-CeO_2 and Pt-CeO_2, could also contribute to the observed differences between supported Pt and supported Rh catalysts.

3.4 Conclusions

Methane partial oxidation over platinum supported on cerium oxide and aluminum oxide was investigated. At low temperatures, the Pt/CeO_2 catalyst gave higher conversion and selectivity, possibly due to redox reactions near the interface of Pt-CeO_2 where lattice oxygen can oxidize adsorbed methane and be replenished by reaction with CO_2 and H_2O. At higher temperatures, the promotion effect of the cerium oxide support becomes less important and the activities and selectivities of both catalysts become comparable. The Pt/CeO_2 catalyst maintained high activity and selectivity throughout variations of the CH_4:O_2 feed ratio from 1.7 to 2.3 while the Pt/Al_2O_3 catalyst had lower activity under methane-rich conditions ($CH_4/O_2 = 2.3$). The redox reactions of the support near the metal-oxide interface could also contribute to the higher activity of Pt/CeO_2 in methane reforming by carbon dioxide.

References

[1] A.T. Ashcroft, A.K. Cheetham, J.S. Foord, M.L.H. Green, C.P. Grey, A.J. Murrell, P.D.F. Vernon, Nature 344 (1990) 319.

[2] A.K. Bhattacharya, J.A. Breach, S. Chand, D.K. Ghorai, A. Hartridge, J. Keary, K.K. Mallick, Appl. Catal. A 80 (1992) L1.

[3] Y. Boucouvalas, Z.L. Zhang, X.E. Verykios, Catal. Lett. 40 (1996) 189.

[4] V.R. Choudhary, A.S. Mamman, S.D. Sansare, Angew. Chem. Int. Ed. Engl. 31 (1992) 1189.

[5] V.R. Choudhary, A.M. Rajput, B. Prabhakar, J. Catal., 139 (1993) 326.

[6] Y.L. Chu, S.B. Li, J.Z. Lin, J.F. Gu, Y.L. Yang, Appl. Catal. A 134 (1996) 67.

[7] D. Dissanayake, M.P. Rosynek, K.C.C. Kharas, J.H. Lunsford, J. Catal. 132 (1991) 117.

[8] D.A. Hickman, L.D. Schmidt, J. Catal. 138 (1992) 267.

[9] D.A. Hickman, E.A. Haupfear, L.D. Schmidt, Catal. Lett. 17 (1993) 233.

[10] P.D.F. Vernon, M.L.H. Green, A.K. Cheetham, A.T. Ashcroft, Catal Lett. 6 (1990) 181.

[11] A. Trovarelli, Catal. Rev. 38 (1996) 439.

[12] H.C. Yao, Y.F.Y. Yao, J. Catal. 86 (1984) 254.

[13] B. Harrison, A.F. Diwell, C. Hallett, Platinum Metals Rev. 32 (1988) 73.

[14] M. Ozawa, M. Kimura, J. Mater. Sci. Lett. 9 (1990) 291.

[15] A.F. Diwell, R.R. Rajaram, H.A. Shaw, T.J. Truex, Stud. Surf. Sci. Catal. 71 (1991) 139.

[16] H.S. Gandhi, M. Shelef, Stud. Surf. Sci. Catal. 30 (1987) 199.

[17] R.K. Herz, J.A. Sell, J, Catal. 94 (1985) 166.

[18] G. Kim, Ind. Eng. Chem. Prod. Res. Dev. 21 (1982) 267.

[19] T.C. Schlatter, P.J. Mitchell, Ind. Eng. Chem. Prod. Res. Dev. 19 (1980) 288.

[20] M. Weibel, F. Garin, P. Bernhardt, G. Maire, M. Prigent, Stud. Surf. Sci. Catal. 71 (1991) 195.

[21] T. Bunluesin, R.J. Gorte, G.W. Graham, Appl. Catal. B 15 (1998) 107.

[22] R. Craciun, B. Shereck, R.J. Gorte, Catal. Lett. 51 (1998) 149.

[23] S. Sharma, S. Hilaire, J.M. Vohs, R.J. Gorte, H.W. Jen, J. Catal. 190 (2000) 199.

[24] K. Otsuka, T. Ushiyama, I. Yamanaka, Chem. Lett. (1993) 1517.

[25] K. Otsuka, E. Sunada, T. Ushiyama, I. Yamanaka, Stud. Surf. Sci. Catal. 107 (1997) 531.

[26] K. Otsuka, Y. Wang, E. Sunada, I. Yamanaka, J. Catal. 175 (1998) 152.

[27] P. Pantu, K. Kim, G.R. Gavalas, Appl. Catal. A 193 (2000) 203.

[28] E. Ruckenstein, H.Y. Wang, J. Catal. 187 (1999) 151.

[29] M.S.G. Baythoun, F.R. Sale, J. Mater. Sci. 17 (1982) 2757.

[30] D. Dissanayake, M.P. Rosynek, J.H. Lunsford, J. Phys. Chem. 97 (1993) 3644.

[31] K. Otsuka, M. Hatano, A. Morikawa, J. Catal. 79 (1983) 493.

[32] C. Padeste, N.W. Cant, D.L. Trimm, Catal. Lett. 18 (1993) 305.

Table 3.1 BET surface areas and specific rates of propene hydrogenation and estimated platinum dispersion of fresh and used samples of 0.5wt% Pt/CeO_2 and 0.5wt% Pt/Al_2O_3 catalysts

Catalyst	Total surface area (m^2/g)	Rate of propene hydrogenation[a] (μmol g^{-1} s^{-1})	Pt dispersion by propene hydrogenation[b] (%)	Pt dispersion by H_2 chemisorption[c] (%)	Pt dispersion by CO chemisorption[c] (%)
Pt/CeO_2 (fresh)	40	22	69	-	-
Pt/CeO_2 (used)[1]	-	9.5	30	-	-
Pt/CeO_2 (used)[2]	12	4.4	14	-	-
Pt/Al_2O_3 (fresh)	268	11	35	39	28
Pt/Al_2O_3 (used)[1]	-	10	34	-	-
Pt/Al_2O_3 (used)[2]	157	8.4	27	24	19

The used sample means that it was used for methane oxidation with the diluted 2:1 CH_4-O_2 feed for 2 h (1) at 600°C, and (2) at 700°C.

[a] Specific rate of propene hydrogenation was measured at 0°C under differential conditions using a feed of 10% propene, 10% H_2 in He at 50 ml/min

[b] The dispersion was calculated based on a conversion factor deduced from Pt dispersion measured by chemisorption of H_2 and the rate of propene hydrogenation.

[c] Chemisorption was measured at room temperature using dynamic pulse method.

Table 3.2 Methane partial oxidation on 50 mg of 0.5% Pt/CeO_2 or 0.5% Pt/Al_2O_3 catalysts using undiluted methane-oxygen feed at 110-120 ml/min flowrate

Furnace temperature (°C)	CH_4/O_2 feed molar ratio	0.5% Pt/CeO_2				0.5% Pt/Al_2O_3			
		CH_4 conversion (%)	CO selectivity (%)	H_2 selectivity (%)	H_2:CO ratio	CH_4 conversion (%)	CO selectivity (%)	H_2 selectivity (%)	H_2:CO ratio
400	1.7	75	70	88	2.5	70	77	79	2.1
500	1.7	80	76	89	2.3	81	79	86	2.2
600	1.7	90	82	93	2.3	87	82	90	2.2
400	1.9	71	70	89	2.6	67	77	82	2.1
500	1.9	76	77	91	2.4	72	79	86	2.2
600	1.9	83	84	94	2.2	78	82	91	2.2
400	2.3	58	68	92	2.7	42	67	60	1.8
500	2.3	63	76	93	2.4	45	71	70	2.0
600	2.3	69	84	95	2.2	52	77	79	2.0

The oxygen conversion was always 100%.

Table 3.3 Methane partial oxidation on 50 mg of 0.5% Pt/CeO_2 or 0.5% Pt/Al_2O_3 catalysts using diluted feed at 50 ml/min flowrate and composition CH_4:O_2 = 1.8-2, He:CH_4 = 8.5

Catalyst	Temperature (°C)	CH_4 conv. (%)	CO select. (%)	H_2 select. (%)	H_2/CO ratio	Degree of reduction (%)	Carbon deposit (%)
0.5% Pt/CeO_2	600	69	79	88	2.2	11	0.0007
	650	82	91	93	2.0	12	0.0005
	700	95	94	94	2.0	15	0.0008
0.5% Pt/Al_2O_3	600	53	60	72	2.4	-	0.0059
	650	72	84	89	2.1	-	0.0004
	700	91	95	95	2.0	-	0.0003
Equilibrium state	600	75	82	92	2.2	-	-
	650	86	92	96	2.1	-	-
	700	92	96	98	2.0	-	-

Oxygen conversion was always 100%; the equilibrium state was calculated based on CH_4:O_2 = 2 and without allowing carbon formation.

Table 3.4 Methane partial oxidation on 10 mg of 0.5% Pt/CeO_2 or 0.5% Pt/Al_2O_3 catalysts using diluted feed CH_4:O_2 = 1.8-2, He:CH_4 = 8.5 at 50 ml/min flowrate

Catalyst	Temperature (°C)	CH_4 conv. (%)	CO select. (%)	H_2 select. (%)	H_2/CO ratio
0.5% Pt/CeO_2	600	53	64	72	2.2
	700	74	85	86	2.0
0.5% Pt/Al_2O_3	600	39	57	42	1.5
	700	70	87	85	2.0

Oxygen conversion was 100% for both catalysts.

Table 3.5 Carbon dioxide reforming of methane on 50 mg of 0.5wt% Pt/CeO_2 or 0.5wt% Pt/Al_2O_3 catalysts using feed CH_4:CO_2:He = 1:1:8 at 50 ml/min flowrate

Catalyst	Temperature (°C)	CH_4 conversion (%)	CO_2 conversion (%)
0.5% Pt/CeO_2	600	56	64
	700	89	92
0.5% Pt/Al_2O_3	600	27	34
	700	67	73
Equilibrium state	600	63	72
	700	88	92

Chapter 4

A Multiple Microreactor System for Parallel Catalyst Testing

Submitted for publication in AIChE Journal

A Multiple Microreactor System for Parallel Catalyst Testing

Piboon Pantu and George R. Gavalas

Division of Chemistry and Chemical Engineering, California Institute of Technology, Pasadena, CA 91125

Abstract

A system containing nine catalytic microreactors for parallel testing of heterogeneous catalysts is described. The catalyst samples are prepared in the form of thin films by dip-coating thin quartz rods with solutions of suitable composition. The catalyst-coated rods are placed within thin tubes housed inside a single wider tube and heated in an electrical furnace. A multiposition valve serves to conduct the reaction products sequentially from each microreactor to a mass spectrometer for analysis. The system was tested with the reaction of methane reforming with carbon dioxide over $Pt/Ce_{1-x}Gd_xO_{2-0.5x}$ and $Pt/Ce_{1-x}Sm_xO_{2-0.5x}$ at 650°C and 700°C. The individual catalysts were characterized by X-ray analysis, and induction-coupled plasma mass spectrometry for catalyst mass and elemental composition. The measurements showed that Pt/CeO_2 had the highest activity among the series of catalysts tested and, generally, the activity increased with the cerium oxide content. After exposure to the feed stream for 2-3 h at 700°C, most catalysts suffered significant deactivation with the exception of the mixed oxides with 25-85% samarium oxide that maintained relatively stable activity.

4.1 Introduction

Parallel processing techniques allow large numbers of materials with systematically varying composition to be prepared and tested simultaneously resulting in large increases of productivity in catalyst discovery and development. Initially developed in medicinal chemistry research, such techniques have been recently introduced to the development of heterogeneous catalysts and other solid state materials. Sputtering and physical masking techniques originally proposed by Hanak (1970) were recently used for rapid synthesis of thin film catalyst "libraries" (Xiang et al. 1995; Cong et al. 1999). Conventional catalyst preparation by co-precipitation and impregnation can also be carried out in a high-throughput fashion with the aid of an automatic liquid dispenser (Reddington et al. 1998; Senkan and Ozturk 1999). Parallel screening for catalyst activity has been carried out by optical techniques such as IR thermography (Moates et al. 1996; Holzwarth et al. 1998; Haap et al. 1998; Snively et al. 2000), resonance-enhanced multiphoton ionization (Senkan and Ozturk 1999), and laser-induced fluorescence imaging (Su and Yeung 2000). More commonly, sequential measurement by mass spectrometry is used to determine product distribution (Cong et al. 1999; Orschel et al. 1999). Sequential rather than parallel measurement of catalytic activity and selectivity does not detract from the value of the parallel processing techniques in as much as the time for a single mass spectrometric measurement, often taking less than one minute, is much shorter than the several hours taken by preparation, mounting in a reactor, calcination, reduction and other conditioning needed in conventional catalyst preparation and testing.

The need for convenient placement of catalysts in reactors for parallel testing has been approached by different designs. Systems similar in design to conventional reactors have been used by Hoffmann et al. 1999 and Perez-Ramirez et al. 2000. Senkan et al. (1999) developed an array of reactor channels machined in an alumina block capable of accommodating on the order of 100 different catalysts. An x-y-z computer-controlled mechanism was used to move the reactor so that the product from different channels could be sampled sequentially by a fixed mass spectrometer probe. Several sophisticated instruments for high throughput catalyst testing are now commercially available. Nevertheless, there is also need for simple, low-cost, multireactor designs for use in academic and industrial laboratories.

In this paper, a multireactor design is described that is suitable for testing certain multicomponent oxide catalysts, zeolite catalysts, and supported metal catalysts. The system contains nine tubular microreactors operating in parallel. The catalysts are prepared as thin films coated on quartz or other ceramic rods, although it is also possible to use powdered samples. The coated rod geometry facilitates catalyst preparation and loading and unloading in the reactors. The multireactor system is tested with the methane-carbon dioxide reaction over platinum supported on rare earth catalysts. This reaction was chosen based on previous work of methane reforming by carbon dioxide on ceria supported noble metals (Craciun et al. 1998; Sharma et al. 2000; Wang and Lu 1998; Xu et al. 1999). Addition of another rare earth oxide to cerium oxide was considered a possible means of increasing oxygen mobility and catalytic activity.

4.2 Experimental

4.2.1 Catalyst preparation

Catalyst samples were prepared by dip-coating thin layers of mixed cerium-gadolinium or cerium-samarium oxides on quartz rods (1 mm diameter) and subsequently adding the metal also by dip-coating. Prior to coating, the quartz rods were roughened with sand paper and cut into pieces 4 cm long, cleaned with water, and finally cleaned with acetone in an ultrasonic bath. Mixed rare earth solutions were prepared by using the citrate complexation technique (Baythoun et al. 1982). Individual solutions of the metal precursors, $Ce(NO_3)_3 \cdot 6H_2O$ (Alfa, 99.5%), $Gd(NO_3)_3 \cdot 6H_2O$ (Alfa, 99.9%), or $Sm(NO_3)_3 \cdot 6H_2O$ (Alfa, 99.9%), were prepared by dissolving equal molar amounts of the metal precursor and citric acid in ethanol to a 0.77 M metal concentration. Mixed solutions of cerium with 0, 10, 25, 40, 55, 70, 85, and 100% gadolinium or samarium were prepared by mixing specified amounts of the metal solutions in small vials to a total volume of 3 ml. The mixed solutions were vigorously stirred for 2 h and then 1ml of 7% (wt/v) ethyl cellulose solution in ethanol was added to the solutions to increase viscosity and binding affinity for coating. The vials were subsequently placed in a multi-well block while the quartz rods were vertically placed in another block in corresponding positions. The quartz rods were then immersed in the solutions for 30 seconds after which the vial block was lowered removing the solutions at a controlled speed of 6.4 cm/min. The coated rods were dried at room temperature for 4 h, further dried at 120°C for 2 h, and calcined at 600°C in air for 4 h resulting in thin films of white oxides. Platinum was added to the coated films by a similar dip-coating procedure using a solution of 0.007 M platinum ($PtCl_4$, Alfa 99.9%) with 3% (wt/v) ethyl cellulose in ethanol and using a pulling speed of 1.2 cm/min. The coated rods were left overnight at room temperature for drying. Each rod had a coated section 2 cm long and a bare section about 1.5 cm long.

4.2.2 Catalyst characterization

X-ray powder diffraction analysis of the coated catalysts was carried out using a Scintag Pad V diffractometer with Cu-Kα radiation. Inductively coupled plasma mass spectrometry (ICP-MS, Perkin-Elmer/Sciex Elan 5000A) was used for elemental analysis to check the consistency of catalyst loading on the coated rods. Powdered samples prepared by drying coating solutions and calcining them at 600°C for 4 h were characterized for BET surface area using a Micromeritics ASAP 2000 instrument.

4.2.3 Reactor configuration

The reactor system contained 10 quartz tubes (4 mm O.D., 2 mm I.D.) placed inside a 2.5 cm O.D. quartz cylinder and held in place by a custom-made Teflon adapter (Fig. 4.1a). One of the tubes was used to house a thermocouple for controlling the temperature, while the other tubes were loaded with the catalyst rods having the non-coated ends resting on the bottom of the reactor system (see Fig. 4.1a inset). The quartz cylinder was placed in a tubular furnace such that the top of the cylinder remained outside of the furnace and was close to ambient temperature. The feed stream was introduced through a common inlet at the top of the quartz cylinder, entered the individual microreactors at the bottom, and exited at the top. A 10-position valve was used to conduct the product of a particular reactor to a valve equipped with a sample loop for injecting 0.5 ml pulses of the selected stream to a mass spectrometer (UTI 100C) for analysis (Fig. 4.1b). Before testing a new batch of catalysts, the reactor tubes were cleaned with 17% nitric acid in an ultra sonic bath and rinsed with water.

4.2.4 Reaction conditions

The reactor system was heated to 600°C at a heating rate of 10°C/min in an oxygen flow of 50 ml/min and kept at that temperature for 30 minutes. The temperature was then raised to 650°C at 2.5°C/min and the system was purged with helium (50 ml/min) for 1 h before switching to a reactant flow of 1:1 CH_4:CO_2 at 30 ml/min. The product composition was monitored for 1 h at 650°C after which the reactor was heated to 700°C at 2.5°C/min and the product composition was measured at that temperature for 3 h. The CO yield was calculated and used as an indication of catalyst activity.

$$\text{CO yield}\,(\%) = 100 \times \frac{[\text{CO}]}{[\text{CH}_4]+[\text{CO}_2]+[\text{CO}]} \qquad (4.1)$$

where [CO], [CH_4],and [CO_2] are the gaseous concentrations in the product stream.

4.3 Results and discussion

4.3.1 Catalyst characterization

The catalyst films appeared to be very thin and uniform. X-ray diffraction analysis showed characteristic peaks similar to those of bulk oxides although the peaks were very weak due to the very small catalyst loading in each sample. Elemental analysis on replicate samples using ICP-MS revealed that the sample rods contained 64±4 μg of catalyst each, while the platinum content was 0.74±0.04 wt% of the coating. Due to the very small catalyst loading on each rod, direct measurement of surface area was not possible. Surface areas of catalyst samples were estimated to be less than 10 m^2/g based on values measured with powder samples obtained by drying the coating solutions.

4.3.2 Reactor characterization

Measurement of temperature in different microreactor tubes showed uniformity within 5°C. Measurements of the flowrate through seven of the tubes gave equal values within ±5%, but the other three tubes had significantly lower or higher flow rate. The unequal flow in these three tubes was likely due to differences in the constrictions inside the 10-position valve. Therefore, only seven reactor tubes, those with uniform flow rates, could be used for catalyst testing in this particular system. Of the three tubes having different flowrates, one was used for blank run, and one for inserting the thermocouple for furnace temperature control. Measurements of catalyst activity for the last tube gave considerably higher conversion due to lower flowrate.

4.3.3 Catalyst testing

Preliminary experiments using identical Pt/CeO_2 catalysts in each reactor gave conversions varying less than ±20%. Runs using rods coated with cerium oxide without platinum and with unsupported platinum gave very low conversions. The very low catalyst activity in the first case could be explained by the absence of the component responsible for methane activation, and in the second case by the very low dispersion of the unsupported metal. Bitter et al. (1997) reported that unsupported platinum black and platinum supported on silica had very low activity whereas platinum supported on alumina and zirconia had very high activity.

Activities of $Pt/Ce_{1-x}Gd_xO_{2-0.5x}$ catalysts for methane reforming with carbon dioxide were tested in the multireactor system at 650°C and 700°C and the CO yields obtained are plotted against the gadolinium content in Figure 4.2. In all cases, selectivity to hydrogen was low, consistent with the low selectivity to hydrogen at low CH_4 conversion reported by Bradford and Vannice (1998). Because of the difficulty of accurately measuring the low levels of hydrogen, catalyst activity was characterized by the yield of CO which was higher and easier to measure. At 650°C, all catalysts showed induction periods of approximately 1 h during which conversion increased and reached a maximum after which it slowly declined to a steady level. Generally, the activity decreased with increasing gadolinium content and was highest for the Pt/CeO_2 catalyst. After the reaction temperature was raised to 700°C, the catalysts with high cerium or high gadolinium content reached their maximum conversion level within 10 minutes but the catalysts with intermediate composition of the mixed oxides took 40-50 minutes to reach the maximum. A trend of decreasing activity with increasing gadolinium content was also observed at 700°C. At this temperature, all catalysts underwent gradual deactivation reaching after 1-2 h significantly lower but steady activities.

The CO yields from reaction over $Pt/Ce_{1-x}Sm_xO_{2-0.5x}$ at 650°C and 700°C are presented in Figure 4.3. At 650°C, the Pt/CeO_2 catalyst had significantly higher activity than the catalysts containing samarium oxide. Catalysts with 40-70% samarium content gave very low CO yields and possibly were not fully activated at 650°C within the 1 h of reaction. After 1 h of exposure to the reactant stream at 700°C, the catalysts containing

40-70% samarium became activated giving yields of CO only slightly lower than those obtained with Pt/CeO_2. Interestingly, catalysts with at least 25% samarium oxide maintained relatively constant activity for 2-3 h at 700°C, while Pt/CeO_2 underwent significant deactivation within the same period.

The induction time to maximum conversion is correlated with the reducibility of the support so that catalysts supported on mixed oxides, having higher oxygen ion mobility and being more readily reducible, had significantly longer induction time than the catalysts supported on the pure oxides. However, the mechanism of this activation could not be inferred from these limited experiments. Long induction periods for the same reaction were reported by Wang and Ruckenstein (2000) for rhodium supported on cerium or zirconium oxides. These authors suggested that the long induction time could be due to reconstruction of metal particles and migration of partially reduced support oxides.

Replicate runs showed reproducible trends of catalytic activities for the Pt/$Ce_{1-x}Gd_xO_{2-0.5x}$ and Pt/$Ce_{1-x}Sm_xO_{2-0.5x}$ catalysts although the absolute values of the CO yield sometimes varied. This variation could be due to small variation of catalyst mass and uneven flow distribution. In addition, the long induction time could also cause some differences in yields that are measured within a limited time period.

4.3.4 Extensions

The loading of rare earth or other oxide catalysts can be significantly increased, if desired, by using instead of the glass rods porous α-Al_2O_3 rods, and instead of dip-coating applying the solution by impregnation. Rods of porous alumina can also be used directly as metal supports using conventional impregnation. Another way to vary the catalyst loading is by changing the viscosity and/or concentration of coating solutions or the coating withdrawal speed. For example, using 8% (wt/v) poly vinyl butyral instead of ethyl cellulose (increasing the viscosity of the coating solution from 30 cps to 180 cps), the catalyst loading on each rod was increased to 120 μg.

The multitube design can be modified to accommodate a much larger number of tubes. Increasing the diameter of the surrounding tube (see Figure 4.1) from 2.5 to 7.5 cm will allow as many as 100 microreactor tubes to be accommodated. Automatic liquid dispensing will be essential for preparing a large number of solutions. A combination of multiposition valves will permit sequential sampling all microreactors. Alternatively, a movable capillary probe may be inserted sequentially in the microreactors to draw product for mass spectrometry. In the case of a larger surrounding tube, uniform temperature can be achieved by preheating the feed gas before introduction into the surrounding cylinder.

4.4 Conclusions

A system of nine parallel microreactors was constructed that permits convenient catalyst preparation and loading in the form of thin films coated on quartz rods. By using a suitable polymer, the viscosity of all coating solutions can be raised to the same level guarantying uniform catalyst loading at dip-coating. The solution viscosity and other parameters of coating can be varied to change the catalyst loading. Multi-position valves can be used to conduct the product streams sequentially to a mass spectrometer for analysis. When using such valves, it is necessary to check for uniformity of flowrates through the individual microreactors. The number of individual microreactors can be increased by a factor of 5 or 10 by using a larger number of multiposition valves and preheating the feed to maintain uniform temperature.

The multireactor system was tested with carbon dioxide reforming of methane on a series of Pt/$Ce_{1-x}Gd_xO_{2-0.5x}$ and Pt/$Ce_{1-x}Sm_xO_{2-0.5x}$ catalysts. The coated catalysts showed similar properties to bulk catalysts and gave consistent and adequate activities for comparison purposes. The results showed that the Pt/CeO_2 catalyst had higher activity than the catalysts supported over the mixed oxides. However, mixed samarium-cerium oxide showed a potential benefit of stabilizing catalytic activity although further experiments are needed for verification.

Literature cited

Baythoun, M. S. G. and F. R. Sale, "Production of strontium-substituted lanthanum manganite perovskite powder by the amorphous citrate process," *J. Mater. Sci.*, **17**, 2757 (1982).

Bitter, J. H., K. Seshan and J. A. Lercher, "The state of zirconia supported platinum catalysts for CO_2/CH_4 reforming," *J. Catal.*, **171**, 279 (1997).

Bradford, M. C. J. and M. A. Vannice, "CO_2 reforming of CH_4 over supported Pt catalysts," *J. Catal.*, **173**, 157 (1998).

Cong, P. J., R. D. Doolen, Q. Fan, D. M. Giaquinta, S. H. Guan, E. W. McFarland, D. M. Poojary, K. Self, H. W. Turner and W. H. Weinberg, "High-throughput synthesis and screening of combinatorial heterogeneous catalyst libraries," *Angew. Chem.-Int. Edit.*, **38**, 484 (1999).

Craciun, R., B. Shereck and R. J. Gorte, "Kinetic studies of methane steam reforming on ceria-supported Pd," *Catal. Lett.*, **51**, 149 (1998).

Haap, W. J., T. B. Walk and G. Jung, "FT-IR mapping – A new tool for spatially resolved characterization of polymer-bound combinatorial compound libraries with IR microscopy," *Angew. Chem.-Int. Edit.*, **37**, 3311 (1998).

Hanak, J. J., "The multiple-sample concept in materials research: synthesis, compositional analysis and testing of entire multi component systems," *J. Mater. Sci.*, **5**, 964 (1970).

Hoffmann, C., A. Wolf and F. Schuth, "Parallel synthesis and testing of catalysts under nearly conventional testing conditions," *Angew. Chem.-Int. Edit.*, **38**, 2800 (1999).

Holzwarth, A., P. W. Schmidt and W. E. Maier, "Detection of catalytic activity in combinatorial libraries of heterogeneous catalysts by IR thermography," *Angew. Chem.-Int. Edit.*, **37**, 2644 (1998).

Moates, F. C., M. Somani, J. Annamalai, J. T. Richardson, D. Luss and R. C. Willson, "Infrared thermographic screening of combinatorial libraries of heterogeneous catalysts," *Ind. Eng. Chem. Res.*, **35**, 4801 (1996).

Orschel, M., J. Klein, H. W. Schmidt and W. F. Maier, "Detection of reaction selectivity on catalyst libraries by spatially resolved mass spectrometry," *Angew. Chem.-Int. Edit.*, **38**, 2791 (1999).

Perez-Ramirez, J., R. J. Berger, G. Mul, F. Kapteijn and J. A. Moulijn, "The six-flow reactor technology – A review on fast catalyst screening and kinetic studies," *Catal. Today*, **60**, 93 (2000).

Reddington, E., A. Sapienza, B. Gurau, R. Viswanathan, S. Sarangapani, E. S. Smotkin and T. E. Mallouk, "Combinatorial electrochemistry: A highly parallel, optical screening method for discovery of better electrocatalysts," *Science*, **280**, 1735 (1998).

Senkan, S. M. and S. Ozturk, "Discovery and optimization of heterogeneous catalysts by using combinatorial chemistry," *Angew. Chem.-Int. Edit.*, **38**, 791 (1999).

Senkan, S., K. Krantz, S. Ozturk, V. Zengin and I. Onal, "High-throughput testing of heterogeneous catalyst libraries using array microreactors and mass spectrometry," *Angew. Chem.-Int. Edit.*, **38**, 2794 (1999).

Sharma, S., S. Hilaire, J. M. Vohs, R. J. Gorte and H. W. Jen, "Evidence for oxidation of ceria by CO_2," *J. Catal.*, **190**, 199 (2000).

Snively, C. M., G. Oskarsdottir and J. Lauterbach, "Chemically sensitive high throughput parallel analysis of solid phase supported library members," *J. Comb. Chem.*, **2**, 243 (2000).

Su, H. and E. S. Yeung, "High-throughput screening of heterogeneous catalysts by laser-induced fluorescence imaging," *J. Am. Chem. Soc.*, **122**, 7422 (2000).

Wang, H. Y. and E. Ruckenstein, "Carbon dioxide reforming of methane to synthesis gas over supported rhodium catalysts: the effect of support," *Appl. Catal. A*, **204**, 143 (2000).

Wang, S. B. and G. Q. Lu, "Role of CeO_2 in Ni/CeO_2-Al_2O_3 catalysts for carbon dioxide reforming of methane," *Appl. Catal. B-Environ.*, **19**, 267 (1998).

Xiang, X. D., X. D. Sun, G. Briceno, Y. L. Lou, K. A. Wang, H. Y. Chang, W. G. Wallacefreedman, S. W. Chen and P. G. Schultz, "A combinatorial approach to materials discovery," *Science*, **268**, 1738 (1995).

Xu, G. L., K. Y. Shi, Y. Gao, H. Y. Xu and Y. D. Wei, "Studies of reforming natural gas with carbon dioxide to produce synthesis gas X. The role of CeO_2 and MgO promoters," *J. Mol. Catal. A-Chem.*, **147**, 47 (1999).

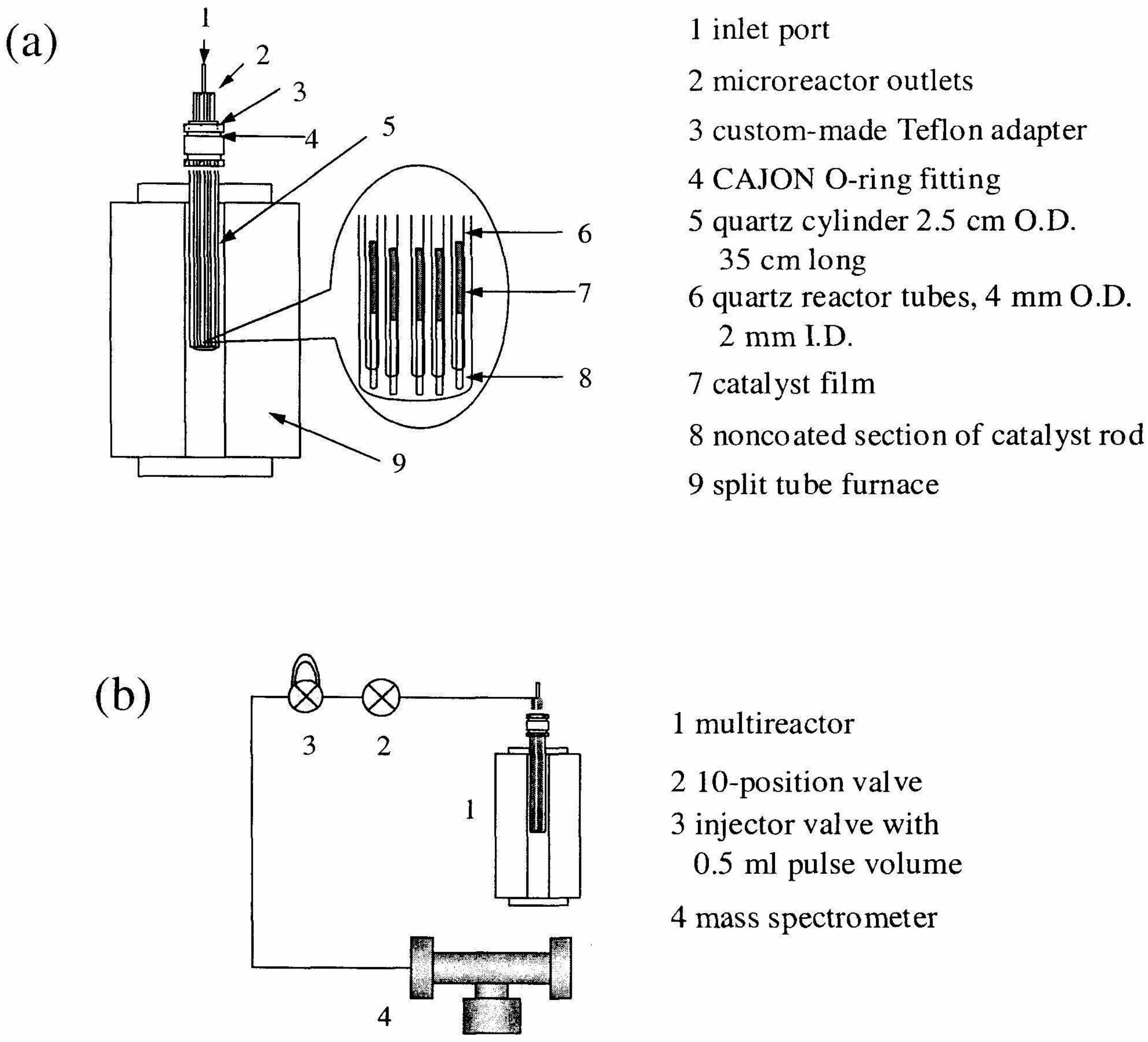

Figure 4.1 (a) Schematic of the multireactor system and (b) product line of the multireactor system.

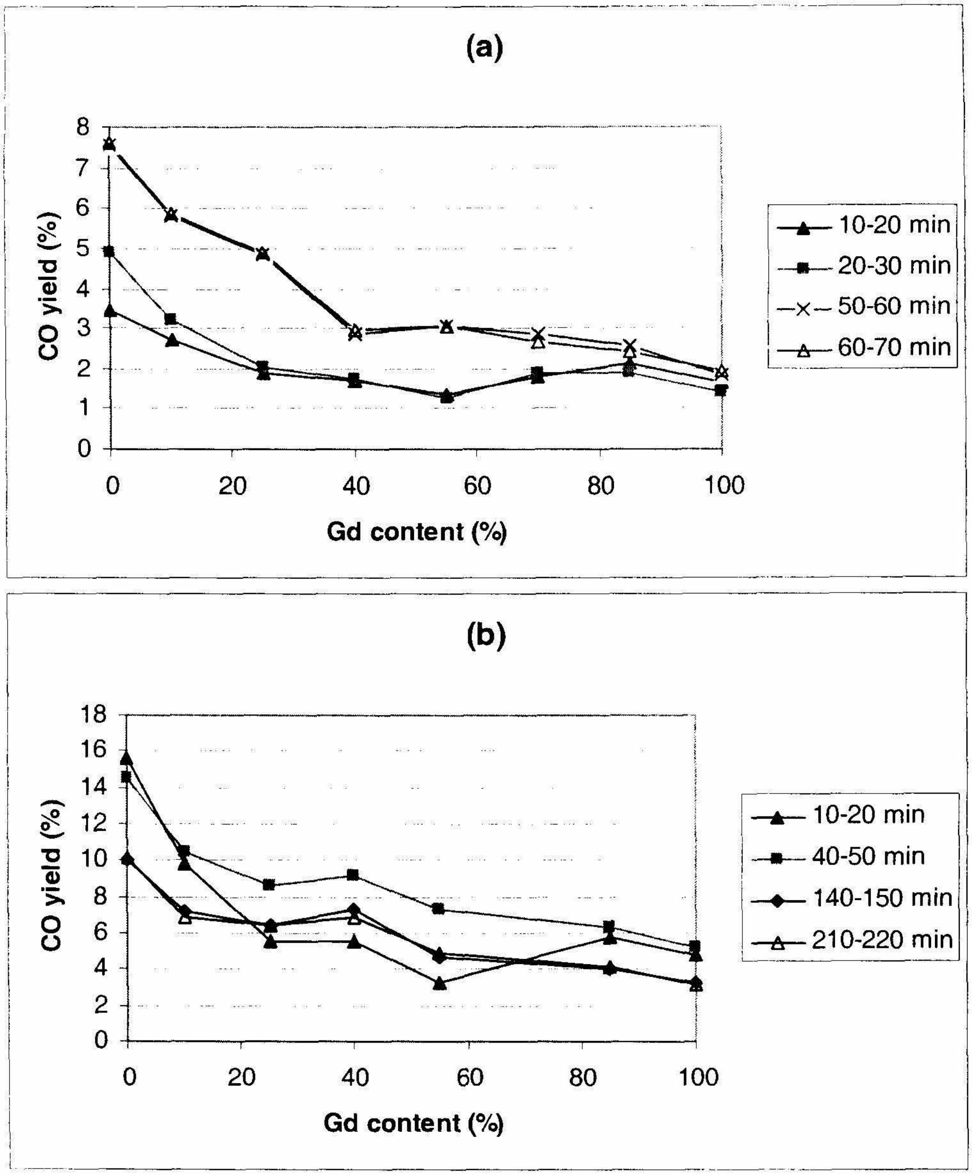

Figure 4.2 CO yield from CH_4 reforming with CO_2 on $Pt/Ce_{1-x}Gd_xO_{2-0.5x}$ at (a) 650°C, (b) 700°C at different times on stream.

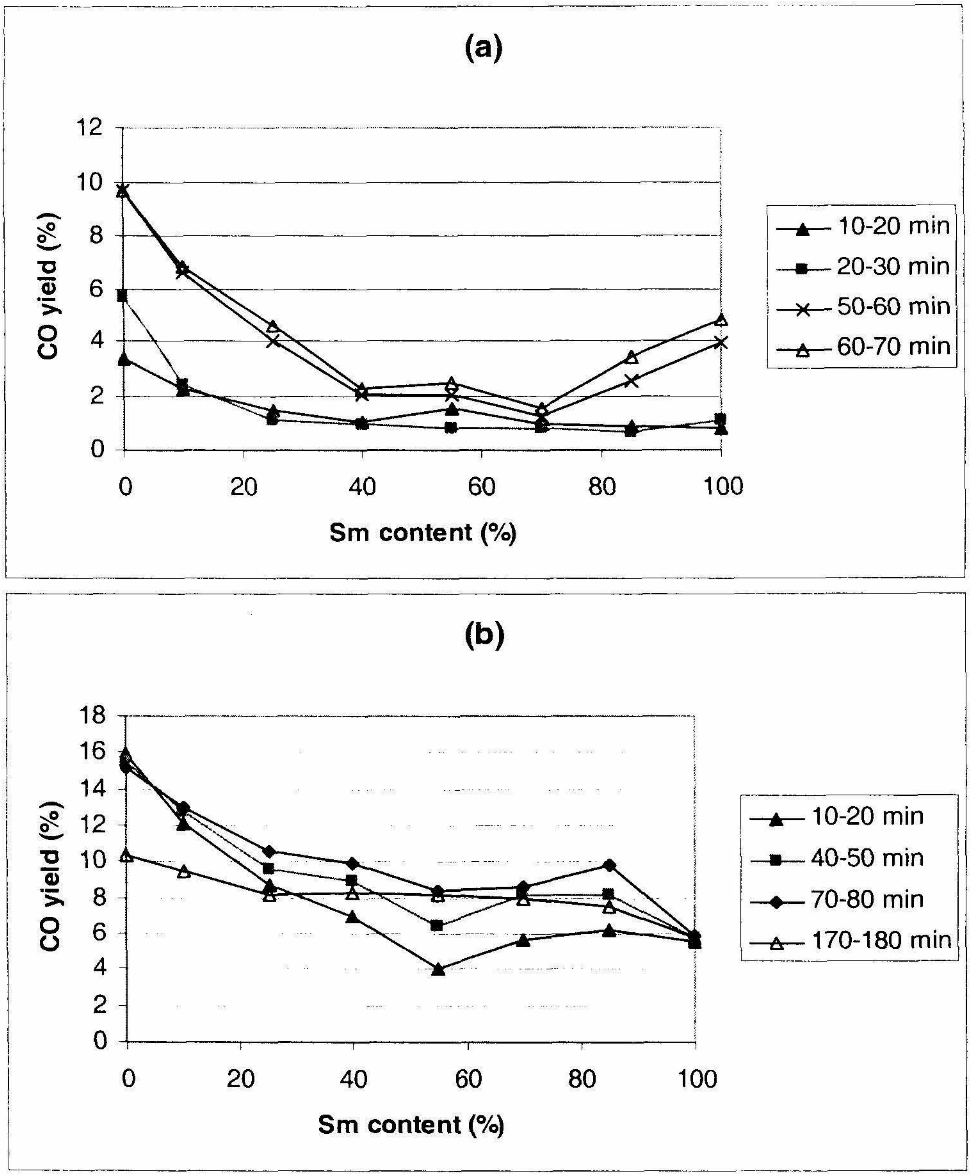

Figure 4.3 CO yield from CH_4 reforming with CO_2 on Pt/$Ce_{1-x}Sm_xO_{2-0.5x}$ at (a) 650°C, (b) 700°C at different times on stream.

Chapter 5

Conclusions

5.1 Conclusions

Methane partial oxidation readily takes place in the absence of gaseous oxygen over platinum or ruthenium supported on CeO_2-ZrO_2. Addition of ZrO_2 to CeO_2 considerably increases the reducibility of the oxide and the rate of methane oxidation but decreases the selectivity to CO and H_2 in the overall product. The oxidation of methane is initially very fast but produces mainly total oxidation products. The higher the ZrO_2 content, the more CO_2 and H_2O produced as the oxide support must be reduced to 10, 40, and 65% degree of reduction for the oxide with 0, 20, and 50% ZrO_2, respectively, before the high selectivity above 90% can be achieved. The oxidation utilizes lattice oxygen of the oxide support therefore the reaction is terminated when the available lattice oxygen is depleted. However, at high methane concentration, carbon deposition occurs so rapidly that the oxidation reaction is terminated by coking of the metal particles before depletion of available lattice oxygen. The fast rate of carbon deposition could be a problem for the application of this catalyst but by adjusting the feed ratio of solid oxide to methane it may be possible to minimize carbon deposition.

Methane partial oxidation over platinum supported on cerium oxide or aluminum oxide appeared to involve total combustion followed by reforming of the remaining CH_4 with CO_2 and H_2O. At low temperatures, the Pt/CeO_2 catalyst gave higher conversion and selectivity, possibly due to the faster reforming rates enhanced by redox reactions near the interface of Pt-CeO_2 where lattice oxygen can oxidize adsorbed methane and be replenished by reaction with CO_2 and H_2O. At higher temperatures, the promotion effect of the cerium oxide support becomes less important and the activities and selectivities of both catalysts become comparable. The Pt/CeO_2 catalyst also maintained high activity and selectivity throughout variations of the CH_4:O_2 feed ratio from 1.7 to 2.3 while the Pt/Al_2O_3 catalyst had lower activity under methane-rich conditions.

A system of nine parallel microreactors was constructed to facilitate testing of heterogeneous catalysts. The system design permits convenient catalyst preparation and loading in the form of thin films coated on thin quartz rods. By carefully controlling the coating procedure and the concentration and viscosity of the coating solutions, uniform catalyst loading can be attained as well as the amount of catalyst can be adjusted. The number of individual microreactors can be increased by a factor of 5 or 10 using the same reactor design and preheating the feed gas to maintain uniform temperature. The multireactor system was tested with carbon dioxide reforming of methane on a series of platinum supported on cerium-gadolinium or cerium-samarium oxides. The results showed that the Pt/CeO_2 catalyst had the highest activity among the series of catalysts tested. However, mixed samarium-cerium oxide showed a potential benefit of stabilizing catalytic activity although further experiments are needed for verification.